

BLOWN UP BY AN EQUILATERAL: PONCELET TRIANGLES ABOUT THE INCIRCLE AND THEIR DEGENERACIES

MARK HELMAN, RONALDO A. GARCIA, AND DAN REZNIK

ABSTRACT. We tour several harmonious Euclidean properties of Poncelet triangles inscribed in an ellipse and circumscribing the incircle. We also show that a number of degenerate behaviors are triggered by the presence of an equilateral triangle in the family.

CONTENTS

1. Introduction	2
1.1. Article structure	2
2. Preliminaries	5
2.1. Cayley closure condition	5
2.2. Symmetric parametrization	6
3. Remarkable loci	7
3.1. Loci of $X(k)$, $k=2,4,7$	7
3.2. Loci of $X(k)$, $k=3,5,8$	9
3.3. Circular $X(36)$	10
4. Degeneracies	12
4.1. C is vertex of $X(3)$	12
4.2. Invariant aspect ratios: $X(3)$, $X(7)$	13
4.3. Segment $X(5)$	14
4.4. Stationary $X(11)$, $X(80)$	15
4.5. Line $X(36)$	15
4.6. Elliptic $X(59)$	17
5. Envelopes	19
5.1. Circumcircle	19
5.2. Radical axis	21
6. Ellipticity of $X(k)$, $k=1, 7, 8$	23
7. Four special families	23
7.1. Focal- $X(1)$	23
7.2. Iso- $X(2)$	26
7.3. Focal- $X(4)$	27
7.4. Iso- $X(7)$	29
Acknowledgements	30
Appendix A. Affine triples	30
Appendix B. Locus behaviors	31
Appendix C. The Contact family	31
Appendix D. Semiaxes of the $X(7)$ locus	35
Appendix E. Table of symbols	37
References	37

1. INTRODUCTION

Poncelet's porism is a 1d family of n -gons with vertices on an 'outer' conic \mathcal{E} and with sides tangent to an 'inner' conic \mathcal{E}_c (also called the 'caustic'). For such a porism to be admitted, \mathcal{E} and \mathcal{E}_c must be positioned in \mathbb{R}^2 so as to satisfy 'Cayley's condition' [7]. While the porism is a projective statement – most conic pairs can be projected to two circles where the 'Poncelet map' is linearized, – we have found that Poncelet triangles are a wellspring of interesting Euclidean phenomena.

Consider when either conic can be a circle or a generic ellipse. Referring to Figure 1, we obtain the following four combinations:

- (1) Both conics are circles: this is Chapple's porism [3]. Loci loci of its *triangle centers*, e.g., incenter X_1 , barycenter X_2 , circumcenter X_3 , orthocenter X_4 (the X_k notation, used here, follows [18]), have been studied in [13, 14, 21, 26]. See Figure 2 (left).
- (2) Only \mathcal{E} is a circle. This system, always an affine image of (4), lends itself to a convenient symmetric parametrization, explained below.
- (3) Only \mathcal{E}_c is a circle: the present study is a tour of its manifold harmonious properties.
- (4) No restriction: though Euclidean phenomena are sparser, some are still discernible, e.g., the locus of certain centers are always conics, the locus of barycenter X_2 and orthocenter X_4 always homothetic to \mathcal{E} (see below), etc.

Another special case is that a triangle family interscribed between two *confocal* ellipses (the 'elliptic billiard'), shown in Figure 2 (right). The loci of all four 'Greek centers' of the triangle – incenter, barycenter, circumcenter, orthocenter – sweep ellipses, as proved in [8, 11, 29].

For case (3), studied here, we start by identifying triangle centers whose loci are conics. In [17] we show that the locus of a triangle center which is a fixed linear combination of the barycenter and the orthocenter is a sufficient condition for that center to sweep a conic. Nevertheless, other centers may still sweep conics for some choices of conic pairs. Still lacking a predictive theory for those, we use numerical methods to pinpoint these, as in [11].

We find many curious dependencies between the shape and foci of certain loci and the specifications of both Poncelet conics. A surprising find has been that the presence of a single equilateral triangle in the family triggers degeneracies in certain loci.

1.1. Article structure. We begin with Section 2, describing two algebraic tool-kits used throughout the paper:

- **Section 2.1:** we derive the 'Cayley' condition for closure of a triangle family interscribed between an ellipse \mathcal{E} and a circle \mathcal{K} (center C), and provide an explicit expression for the caustic radius as a function of the ellipse data. We then visualize the quartic C -isocurves of the radius of \mathcal{K} .
- **Section 2.2:** we present a parametrization for Poncelet triangles inscribed in the unit circle in \mathbb{C} which keeps the intrinsic symmetry of the vertices, using the work on 'Blaschke products' from [4]. We then present the generalization to Poncelet families of convex triangles interscribed between any two ellipses as described in [17], and then specialize it to the case where the inner ellipse is a circle, providing explicit formulas.

These are our main results:

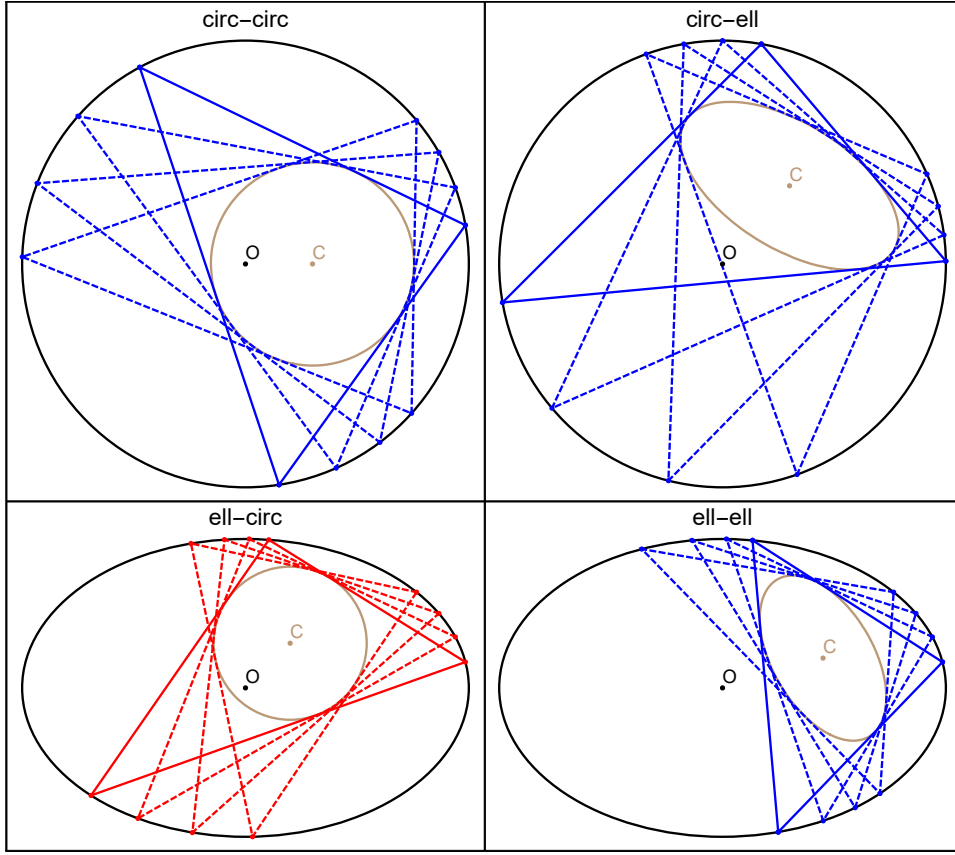


FIGURE 1. **upper left:** outer and inner Poncelet conics $\mathcal{E}, \mathcal{E}_c$ are circles (Chapple's porism); **upper right:** outer \mathcal{E} is a circle; **bottom left:** inner \mathcal{E}_c is a circle (in red since focus of present work); **bottom right:** neither \mathcal{E} nor \mathcal{E}_c is a circle. [Video](#)

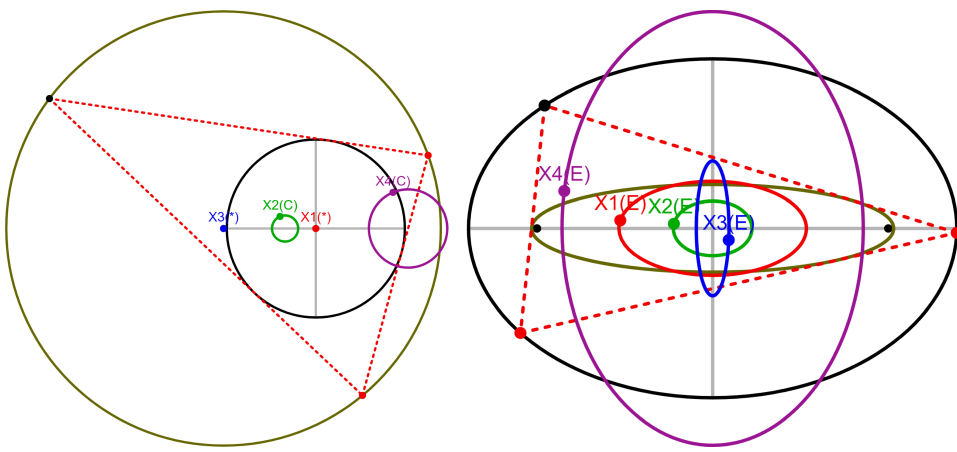


FIGURE 2. **left:** the loci of triangle centers $X_k, k = 1, 2, 3, 4$ over Chapple's porism, studied in [21]. [live](#); **right:** elliptic loci of said triangle centers over the confocal family, studied in [27]. [live](#)

- **Section 3:** we characterize remarkable properties of loci of certain triangle centers, including the barycenter, circumcenter, orthocenter, Euler center, and the Gergonne and Nagel points, labeled in [18] as X_2, X_3, X_4, X_5, X_7 , and X_8 , respectively. The behaviors include:
 - Axis-alignment, concentricity, and homothety with respect to \mathcal{E} .
 - The ‘pinning’ or ‘railing’ of the foci of certain centers to the axes of \mathcal{E} or to the caustic center C .
 - Circularity: for no obvious reason, some centers always trace circles, regardless of C . X_{36} , the inversive image of the incenter (stationary in our case) with respect to the (moving) circumcircle is always a circle. We derive expressions for its center and radius.
- **Section 4:** A series of curious, ‘degenerate’ locus phenomena occurs if the Poncelet family contains an equilateral triangle. This occurs when C is on a special ellipse \mathcal{E}_{eq} which is the locus of the centroids of all equilaterals inscribed in \mathcal{E} , and derived in [34]. We prove the following phenomena:
 - (1) C is a vertex of the locus of X_3 .
 - (2) The locus of X_5 collapses to a segment.
 - (3) The Feuerbach point X_{11} becomes stationary on the incircle, and the reflection of the incenter about it (X_{80}) is pinned to a point on \mathcal{E} .
 - (4) The aspect ratio of the loci of the circumcenter X_3 and the Gergonne point X_7 are invariant over all C on \mathcal{E}_{eq} .
 - (5) The locus of X_{36} becomes a straight line (infinite radius circle).
 - (6) The locus of X_{59} , the ‘isogonal conjugate’ of X_{11} (a type of inversive transformation [36]), normally a high-degree curve, ‘tames down’ to an ellipse which touches \mathcal{E} at a special point.
- **Section 5:** the harmonious envelopes of both the circumcircle and of the (incircle, circumcircle) radical axis are studied. The former is shown to have two circular boundaries centered on the foci of the X_3 locus, and the latter is shown to be always a conic, which degenerates to a parabola if C is on the boundary \mathcal{E}_{eq} . We conjecture that the envelope of said radical axis is a conic if and only if the Poncelet family circumscribes a circle.
- **Section 6:** by comparing several Poncelet triangle families, we conjecture that the loci of X_7 and X_8 can only be ellipses if the caustic is a circle or the pair is confocal.
- **Section 7:** we describe four special triangle porisms about a fixed incircle, that keep key triangle centers stationary: X_1, X_2, X_4 , and X_7 . We also identify their conservations, some of which generalize to $n > 3$ Poncelet porisms.

The following appendices are provided:

- **Appendix A:** a table of ‘affine triples’ used in various calculations involving loci, reproduced from [17, Table 1].
- **Appendix B:** we categorize several dozen triangle centers according to one of six remarkable ‘behaviors’: E-homothety, axis-alignment, focus on C , major (resp. minor) axis through C , and circularity.
- **Appendix C:** we analyze the circle-inscribed ‘contact’ family, showing that some of its phenomena are closely related to those of the original family.
- **Appendix D:** Long expressions for the semiaxes of the locus of the Gergonne point X_7 .

- Appendix E compiles most symbols used in the article.

In [6, p.210] it is said that an experimental discovery approach “offers the possibility in some instances of formalizing the inductive leaps that the mathematical mind takes when confronted with what seems to be, logically speaking, incomplete evidence”. This has certainly been the case for us as most phenomena have been discovered via combination. We include include links to animations of the relevant phenomena in some figure captions as well as links to experiments with our interactive tool [5].

2. PRELIMINARIES

2.1. Cayley closure condition. The Cayley condition specifies whether two ellipses $\{\mathcal{E}, \mathcal{E}_c\}$ admit a Poncelet family of n -gons [7]. Referring to Figure 1 (bottom right), consider a Poncelet triangle family ($n = 3$) inscribed in an ellipse centered at the origin with semiaxis lengths a and b . Let (x_c, y_c) be the center and a_c and b_c be the semi-axes lengths of a ‘caustic’ ellipse \mathcal{E}_c nested within \mathcal{E} , and let θ_c be the angle of its major axis with respect to the ‘horizontal’ major axis of \mathcal{E} .

In the calculations below, $c_c^2 = a_c^2 - b_c^2$. Correcting our own expression in [16, formula (3)]:

Proposition 1. *The Cayley condition for the pair $(\mathcal{E}, \mathcal{E}_c)$ to admit an $n = 3$ family is given by:*

$$(1) \quad \begin{aligned} & (a^4 b_c^4 + a_c^4 c^4 + b^4 b_c^4 - 2a^2 b^2 b_c^4 - 2c^4 a_c^2 b_c^2) c\theta^4 - 8a^2 b^2 c_c^2 x_c y_c s\theta c\theta \\ & + [2c_c^2 (a^2 + b^2) (a^2 y_c^2 - b^2 x_c^2) + 2c_c^2 b^2 a^4 + 2(b^2 b_c^4 - a_c^4 c^4 - b^4 c_c^2) a^2 + 2b_c^2 (a_c^2 c^4 - b^4 b_c^2)] c\theta^2 \\ & + a^4 y_c^4 + b^4 x_c^4 + 2b^2 (a^2 a_c^2 - a^2 b^2 - b^2 b_c^2) x_c^2 + 2a^2 b^2 x_c^2 y_c^2 - 2a^2 (a^2 a_c^2 + a^2 b^2 - b^2 b_c^2) y_c^2 \\ & + (aa_c - ab - bb_c)(aa_c + ab - bb_c)(aa_c - ab + bb_c)(aa_c + ab + bb_c) = 0 \end{aligned}$$

where $c\theta = \cos \theta$, $s\theta = \sin \theta$.

Henceforth, let $\delta = \sqrt{(b^4 + c^2 y_c^2)(a^4 - c^2 x_c^2)}$. Referring to Figure 1 (bottom left), we specialize this to a circular caustic:

Proposition 2. *The radius r for an $N = 3$ circular caustic with center at (x_c, y_c) is given by:*

$$r = \frac{b\sqrt{a^4 - c^2 x_c^2} - a\sqrt{b^4 + c^2 y_c^2}}{c^2}$$

Proof. When the caustic is the circle (x_c, y_c, r) , the condition in Equation (1) reduces to a biquadratic on r :

$$c^4 r^4 + 2(b^2 c^2 x_c^2 - a^2 c^2 y_c^2 - a^2 b^2 (a^2 + b^2)) r^2 + (a^2 b^2 - a^2 y_c^2 - b^2 x_c^2)^2 = 0$$

which has four real roots, or four complex roots. The smaller positive root of the above yields a caustic interior to \mathcal{E} . The other positive root $r^* > r$, given by:

$$r^* = \frac{b\sqrt{a^4 - c^2 x_c^2} + a\sqrt{b^4 + c^2 y_c^2}}{c^2}$$

yields a circle which completely encloses or intersects \mathcal{E} , potentially leading to a complex porism. \square

As shown in Figure 3, the expression in Proposition 2 prescribes for the interior of \mathcal{E} a foliation of quartic C -isocurves of caustic radius.

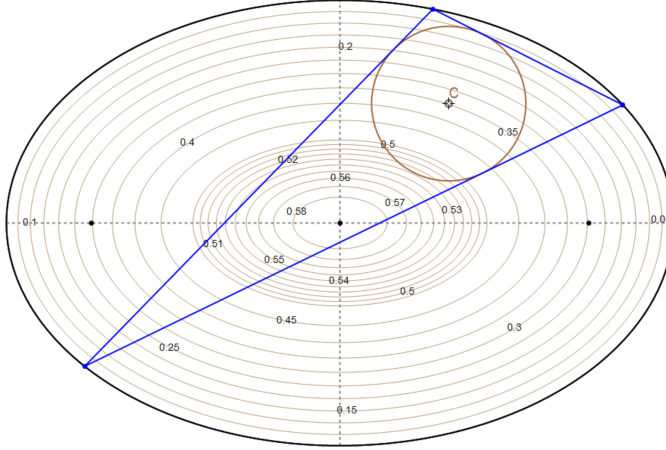


FIGURE 3. The interior of \mathcal{E} is foliated by a family of quartic C -isocurves of caustic radius, $C = X_1$. A particular caustic is shown on the $r = 0.35$ isocurve along with one Poncelet triangle.

2.2. Symmetric parametrization. to do

Identifying \mathbb{R}^2 with \mathbb{C} , we derived in [16, Def. 3] the following parameterization of Poncelet triangle families inscribed in \mathbb{T} , the unit circle centered at the origin, based on the work in [4] on Blaschke products:

Theorem 1. *For any Poncelet family of triangles inscribed in the unit circle \mathbb{T} and circumscribed about an ellipse with foci $f, g \in \mathbb{D}$ (the unit disk), we can parametrize the elementary symmetric polynomials of its vertices $z_1, z_2, z_3 \in \mathbb{T}$ as*

$$\begin{aligned} z_1 + z_2 + z_3 &= f + g + \lambda \bar{f} \bar{g} \\ z_1 z_2 + z_2 z_3 + z_3 z_1 &= f g + \lambda (\bar{f} + \bar{g}) \\ z_1 z_2 z_3 &= \lambda \end{aligned}$$

where λ is a parameter that moves along \mathbb{T} .

In order to generalize this parameterization for any Poncelet family of triangles interscribed between two ellipses, we simply apply an affine transformation that takes the unit circle centered at the origin to the desired outer ellipse. Without loss of generalization, we can assume that the outer ellipse is also centered at the origin and its major axis aligned with the real axis of \mathbb{C} .

As before, let \mathcal{E} and \mathcal{E}_c be the outer and inner ellipses of a Poncelet family of triangles and let a and b be the lengths of the semi-major and semi-minor axes of \mathcal{E} , respectively, where \mathcal{E} is axis-aligned and centered at the origin. We can then use the transformation $T : \mathbb{R}^2 \rightarrow \mathbb{R}^2$ defined by $T(x, y) = (ax, by)$ to transform the unit circle into \mathcal{E} . With a slight abuse of notation, this transformation can also be represented in the complex plane, $T : \mathbb{C} \rightarrow \mathbb{C}$, as $T(z) := \frac{(a+b)}{2}z + \frac{(a-b)}{2}\bar{z}$.

Label the vertices of our general family of Poncelet triangles as $z_1, z_2, z_3 \in \mathcal{E}$. Defining $\mathcal{E}_{pre} := T^{-1}(\mathcal{E}_c)$ and $z'_i := T^{-1}(z_i) \in \mathbb{T}$ for $i \in \{1, 2, 3\}$, we find that the triangles $\{z'_1, z'_2, z'_3\}$ form a Poncelet family interscribed between the unit circle \mathbb{T} and the ellipse \mathcal{E}_{pre} . We can then apply the previous parameterization of the elementary symmetric polynomials in z'_1, z'_2, z'_3 . This allows us to parameterize any symmetric rational function of the vertices z_1, z_2, z_3 of the general Poncelet triangle family as follows:

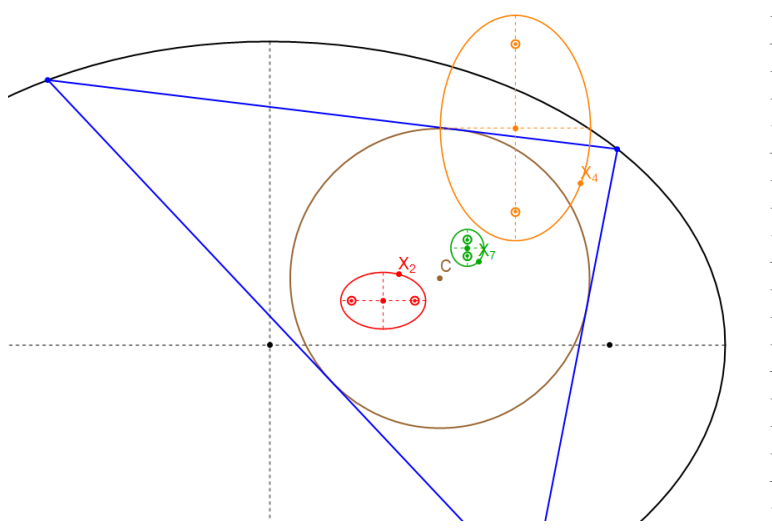


FIGURE 4. Close-up of the first quadrant of \mathcal{E} , showing a Poncelet triangle (blue) and the circular caustic centered on $C = X_1$. Also shown are the loci of the barycenter X_2 (red), orthocenter center X_4 (orange), and Gergonne point X_7 (green). [Video](#)

Let $P : \mathbb{C}^3 \rightarrow \mathbb{C}$ be a symmetric rational function. Our objective is to parameterize the point $P(z_1, z_2, z_3)$. Since P is symmetric on its 3 inputs, the function $P(T(\cdot), T(\cdot), T(\cdot)) : \mathbb{C}^3 \rightarrow \mathbb{C}$ must also be symmetric on its 3 inputs. Restricting T to the unit circle \mathbb{T} , we can write $T : \mathbb{T} \rightarrow \mathcal{E}$ as $T(z) := \frac{(a+b)}{2}z + \frac{(a-b)}{2}\frac{1}{z}$, which is itself a rational function. Thus, $P(z_1, z_2, z_3) = P(T(z'_1), T(z'_2), T(z'_3))$ is a symmetric rational function on z'_1, z'_2, z'_3 . Write $P(z_1, z_2, z_3) = \frac{P_1(z'_1, z'_2, z'_3)}{P_2(z'_1, z'_2, z'_3)}$ where P_1 and P_2 are symmetric polynomials. By the Fundamental Theorem of Symmetric Polynomials, we can express $P_1(z'_1, z'_2, z'_3)$ and $P_2(z'_1, z'_2, z'_3)$ as polynomials in $\sigma_1, \sigma_2, \sigma_3$ where $\sigma_1 := z'_1 + z'_2 + z'_3$, $\sigma_2 := z'_1 z'_2 + z'_2 z'_3 + z'_3 z'_1$, and $\sigma_3 := z'_1 z'_2 z'_3$. Substituting the symmetric parameterization from Theorem [Theorem 1](#), we finally arrive at a parameterization for $P(z_1, z_2, z_3)$ with $\lambda \in \mathbb{T}$ as the parameter, as desired.

3. REMARKABLE LOCI

In this section, let \mathcal{T} (resp. \mathcal{T}_g) denote a family of Poncelet triangles circumscribing a circle (resp. interscribed between two generic conics $\mathcal{E}, \mathcal{E}_c$). In both cases, let the center of the outer conic be the origin and $C = [x_c, y_c]$ denote the caustic's center.

In [\[17, Thm.1\]](#) we showed that if a triangle center X is a fixed linear combination of the barycenter X_2 and the circumcenter X_3 , its locus over any Poncelet family is a conic. Since over \mathcal{T} the incenter X_1 is fixed:

Corollary 1. *Any center which is a fixed linear combination of the incenter X_1 and a another center which sweeps a conic locus will also sweep a conic as its locus.*

3.1. Loci of $X(k)$, $k=2,4,7$. The barycenter X_2 (resp. orthocenter X_4) is the meet-point of lines from each vertex to the opposite side's midpoint (resp. altitude foot). The Gergonne point X_7 is the meet-point of lines from each vertex to the where the opposite side touches the inscribed circle. For more information, see [\[36\]](#).

For next three propositions, refer to Figure 4.

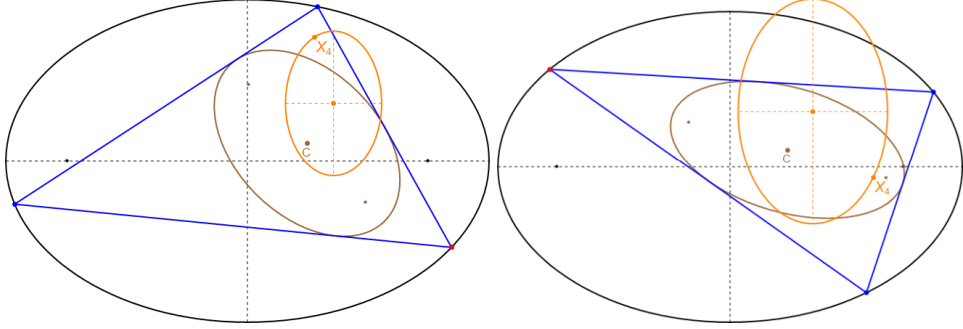


FIGURE 5. **left:** a Poncelet triangle (blue) interscribed between an outer ellipse \mathcal{E} and a generic caustic \mathcal{E}_c , let C be its center. Over the family, the locus of X_4 (orange) is homothetic to a 90° -rotated copy of \mathcal{E} . **right:** another caustic centered at C which closes Poncelet. Notice that the center of the (new) locus of X_4 remains at the same location. [Video](#)

Proposition 3. Over \mathcal{T} , the locus of X_2 is homothetic to \mathcal{E} . Its center C_2 is collinear with the center of \mathcal{E} and the caustic center C . The center C_2 and semi-axis lengths a_2, b_2 are given by:

$$\begin{aligned} C_2 &= \frac{2}{3} [x_c, y_c] \\ a_2^2 &= \frac{-4 ab (a^2 + b^2) \delta - 4 b^4 c^2 x_c^2 + 4 a^4 c^2 y_c^2 + a^2 b^2 (a^4 + 6 a^2 b^2 + b^4)}{9 b^2 c^4} \\ b_2^2 &= \frac{b^2}{a^2} a_2^2 \end{aligned}$$

Note that $a_2/b_2 = a/b$, as claimed.

We note that this is a special case of [30, Thm.1], which states that for any pair of conics admitting a Poncelet family, the loci of both vertex and area centroids sweep conics. For triangles, these are coincident.

Referring to Figure 5, the following has been proved in [15]:

Theorem 2. Over \mathcal{T}_g the locus of X_4 is a conic homothetic to a 90° -rotated copy of \mathcal{E} . The locus center C_4 only depends on a, b of \mathcal{E} and C and is given by:

$$C_4 = \left[\frac{(a^2 + b^2)}{a^2} x_c, \frac{(a^2 + b^2)}{b^2} y_c \right]$$

Proposition 4. Over \mathcal{T} the semiaxis lengths a_4, b_4 of the X_4 locus are given by:

$$a_4^2 = \frac{z_4}{a^2 b^4 c^4}, \quad b_4^2 = \frac{z_4}{b^2 a^4 c^4}$$

where:

$$\begin{aligned} z_4 &= (a^2 + b^2)(a^8 y_c^2 + b^8 x_c^2 - 4a^3 b^3 \delta) + a^8 b^4 + a^6 b^4 (6b^2 - z'_4) + a^4 b^6 (b^2 - z'_4) \\ z'_4 &= x_c^2 + y_c^2 \end{aligned}$$

Proof. CAS. Notice that $a_4/b_4 = a/b$. as required. \square

Let \mathcal{L}_7 denote the locus of the Gergonne point X_7 .

Proposition 5. Over \mathcal{T} , \mathcal{L}_7 is an ellipse with major (resp. minor) axis is parallel to \mathcal{E} 's minor (resp. major axis). The coordinates of its center $C_7 = [x_7, y_7]$ are given by:

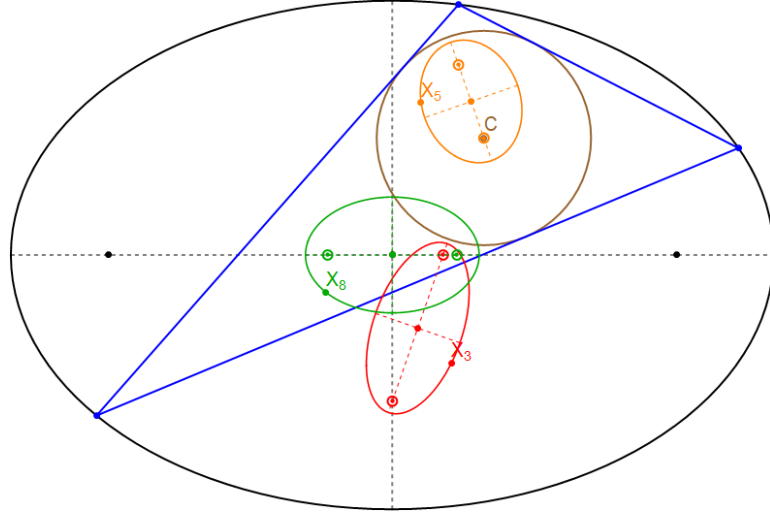


FIGURE 6. A Poncelet triangle (blue) is shown inscribed in an outer ellipse and circumscribing the incircle centered at $C = X_1$. Also shown are the loci of the circumcenter X_3 (red), Euler center X_5 (orange), and Nagel point X_8 (green). [Video 1](#), [Video 2](#)

$$x_7 = \frac{4ax_c (4a^5 + a^3b^2 + ab^4 - a(4a^2 - 3b^2)x_c^2 - ab^2y_c^2 - 3b\delta)}{a^2(4a^2 - b^2)^2 - (4a^2 - 3b^2)^2x_c^2 - a^2b^2y_c^2}$$

$$y_7 = \frac{4by_c (4b^5 + a^2b^3 + a^4b - b(4b^2 - 3a^2)y_c^2 - a^2bx_c^2 - 3a\delta)}{b^2(4b^2 - a^2)^2 - (3a^2 - 4b^2)^2y_c^2 - a^2b^2x_c^2}$$

Furthermore, the ratio of semi-axis lengths a_7/b_7 is given by:

$$\left(\frac{a_7}{b_7}\right)^2 = \frac{y_7 x_c}{x_7 y_c}$$

Proof. to do □

Observation 1. The semi-axis' lengths a_7, b_7 of \mathcal{L}_7 are rather long expressions, appearing in [Appendix D](#).

3.2. Loci of $X(k)$, $k=3,5,8$. The circumcenter X_3 is the center of the circumscribed circle. The Euler center X_5 is the center of the nine-point circle, which passes through the sides' midpoints. The Nagel point X_8 is the meet-point of lines from each vertex to where the opposite touches an excircle. For more information, see [36].

For the next three propositions, refer to [Figure 6](#). Let \mathcal{L}_3 be the (elliptic) locus of X_3 over \mathcal{T} .

Proposition 6. The foci F_3, F'_3 of \mathcal{L}_3 are collinear with C and are each railed to an axis of \mathcal{E} , namely:

$$F_3 = [x_c(1 - (b/a)^2), 0], \quad F'_3 = [0, y_c(1 - (a/b)^2)]$$

Furthermore, the locus semi-axis lengths a_3, b_3 of \mathcal{L}_3 are given by:

$$(2) \quad a_3 = \delta_3(a/b) - \delta'_3(b/a), \quad b_3 = \delta'_3 - \delta_3$$

where $\delta_3 = \frac{\sqrt{b^4 + c^2 y_c^2}}{2b}$ and $\delta'_3 = \frac{\sqrt{a^4 - c^2 x_c^2}}{2a}$.

Observation 2. *In the special case when the circular caustic is concentric with \mathcal{E} , (i) $r = (ab)/(a+b)$, (ii) the invariant circumradius $R = (a+b)/2$, and (iii) X_3 sweeps a circle of radius $(a-b)/2$ concentric with \mathcal{E} [9, Section 3]. If the latter's center is thought of as two coinciding foci, note that each is still on an axis of \mathcal{E} , as required by Proposition 6.*

Let \mathcal{L}_5 denote the (elliptic) locus of X_5 over \mathcal{T} .

Proposition 7. *Ae focus F_5 of \mathcal{L}_5 is at $C = (x_c, y_c)$ and the other F'_5 is given by:*

$$F'_5 = \left[x_c \frac{1 + (b/a)^2}{2}, y_c \frac{1 + (a/b)^2}{2} \right]$$

Furthermore, the semi-axis lengths a_5, b_5 of \mathcal{L}_5 are given by:

$$a_5 = \frac{(a^5 + 3a^3b^2)\delta_3 - (b^5 + 3a^2b^3)\delta'_3}{abc^2}, \quad b_5 = \frac{(3a^3 + ab^2)\delta_3 - (3b^3 + a^2b)\delta'_3}{c^2}$$

where δ_3, δ'_3 are as defined for the locus of X_3 .

Proposition 8. *Over \mathcal{T} , the locus of the Nagel point X_8 is an ellipse homothetic and concentric with \mathcal{E} . Its semi-axis lengths a_8, b_8 are given by:*

$$a_8 = \frac{\sqrt{\delta_8}}{bc^2}, \quad b_8 = \frac{\sqrt{\delta_8}}{ac^2}$$

where: $\delta_8 = (a^3b + ab^3 - 2\delta)^2 + 4c^4x_c^2y_c^2$. Note that $a_8/b_8 = a/b$ as claimed.

Proof. to do □

3.3. Circular X(36). The inversive image of the incenter X_1 with the respect to the circumcircle is called X_{36} on [18]. Referring to Figure 7, the following is a rather surprising phenomenon:

Proposition 9. *Over \mathcal{T} , the locus of X_{36} is a circle. Its center C_{36} is given by:*

$$C_{36} = [x_{36}/z_1, y_{36}/z_1]$$

$$x_{36} = x_c(z_2 - 6a^4b^4 + 6a^4b^2y_c^2 - 3a^2b^6 - 2a^2b^4x_c^2 + 3a^2b^4y_c^2 - 8ab^3\delta + 3b^6x_c^2)$$

$$y_{36} = y_c(3a^6(y_c^2 - b^2) - a^4(6b^4 + b^2(2y_c^2 - 3x_c^2)) - 8a^3b\delta + a^2b^4(b^2 + 6x_c^2 - y_c^2) - 9b^6x_c^2)$$

where:

$$z_1 = z_2 - 2a^4b^4 - 6a^4b^2y_c^2 + a^2b^6 - 6a^2b^4x_c^2 - a^2b^4y_c^2 - 9b^6x_c^2$$

$$z_2 = a^6b^2 - 9a^6y_c^2 - a^4b^2x_c^2$$

Furthermore, the radius r_{36} of the locus X_{36} is given by:

$$\begin{aligned} r_{36} &= \frac{2(\delta_4 z_{36} - \delta'_4 z'_{36})}{a^2b^2c^4 - b^2(a^2 + 3b^2)^2x_c^2 - a^2(3a^2 + b^2)^2y_c^2} \\ z_{36} &= 5ba^4y_c^2 - b^3a^2(a^2 + y_c^2 - x_c^2) + b^5(a^2 + 3x_c^2) \\ z'_{36} &= 5ab^4x_c^2 - a^3b^2(b^2 + x_c^2 - y_c^2) + a^5(b^2 + 3y_c^2) \end{aligned}$$

where $\delta_4 = \sqrt{a^4 - c^2x_c^2}$ and $\delta'_4 = \sqrt{b^4 + c^2y_c^2}$.

Referring to Figure 8:

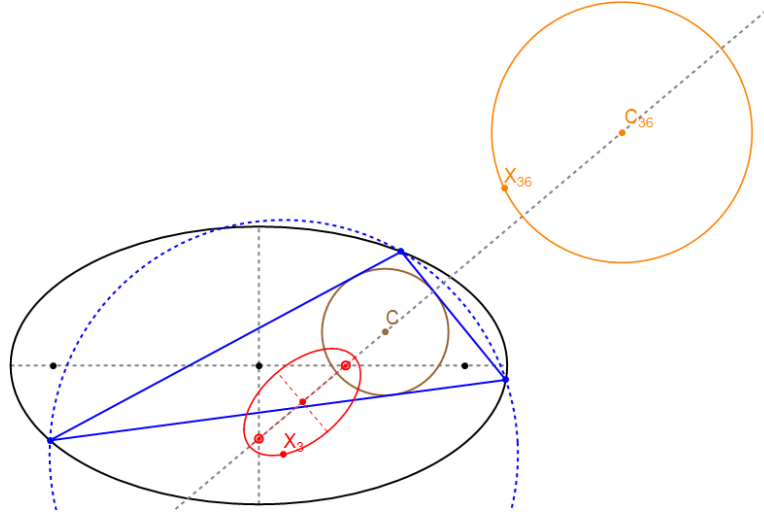


FIGURE 7. The locus of X_{36} , the inversion of $C = X_1$ (fixed) with respect to the (moving) circumcircle (dashed blue), is a circle (orange). Also shown is the elliptic locus of the circumcenter X_3 (red), whose foci F_3, F'_3 lie on the semiaxes of the outer ellipse. Indeed, F_3, F'_3, C, C_{36} are collinear. Note that from the inversion operation, $X_3 X_1 X_{36}$ are dynamically collinear. Indeed, the foci [live](#)

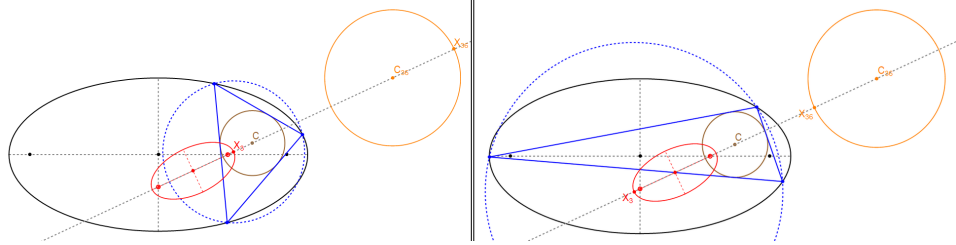


FIGURE 8. The major axis of the X_3 locus passes through the center C_{36} of the circular locus of X_{36} . On the left (resp. right), X_3 is at the major vertex of the locus closest to (resp. farthest from) $C = X_1$, in which case the circumradius is minimized (resp. maximized) and X_{36} is farthest from (resp. closest to) C . [live](#)

Proposition 10. *The major axis of \mathcal{L}_3 passes through the center C_{36} of the X_{36} locus. Furthermore, the circumradius is minimized (resp. maximized) when X_3 is on a major vertex of its locus closest (resp. farthest) from $C = X_1$. At these configurations, the distance $|X_1 X_{36}|$ maximized (resp. minimized), respectively.*

Proof. Direct from Proposition 6 and Proposition 9. □

Referring to Figure 9:

Corollary 2. *Over \mathcal{T} , when C is at the center of \mathcal{E} , the locus of X_{36} is a circle concentric with \mathcal{E} , r_{36} reduces to:*

$$r_{36}^* = \frac{2ab}{a-b}$$

Proof. Direct from setting $x_c = y_c = 0$ in r_{36} (Proposition 9). □

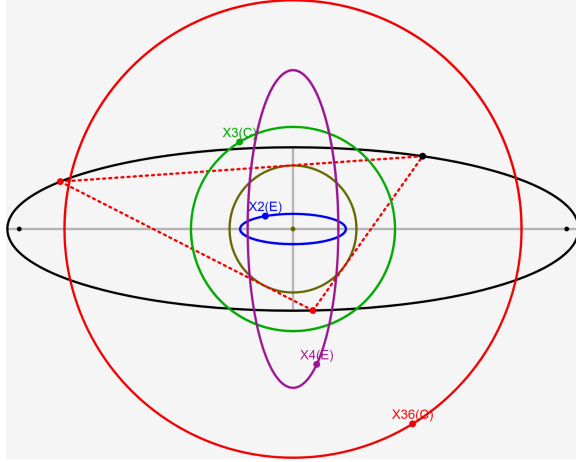


FIGURE 9. With $C = X_1 = [0, 0]$, the locus of X_{36} (red) is a circle concentric with \mathcal{E} . In the figure, $a = 7/2$ and $b = 1$, so $r_{36} = 14/5$. Also shown are the loci of X_2 (blue ellipse), X_3 (green circle) and X_4 (purple ellipse). [live](#)

4. DEGENERACIES

This section described many degeneracies brought about by the ‘presence’ of an equilateral triangle in \mathcal{T} . The locus of centroids of a 1d family of equilateral triangles inscribed in an ellipse $\mathcal{E} = (a, b)$ is an ellipse – henceforth called \mathcal{E}_{eq} – concentric and axis-aligned with \mathcal{E} , whose semi-axes a_{eq}, b_{eq} are given by [32, 34]:

$$a_{eq} = \frac{a c^2}{a^2 + 3b^2}, \quad b_{eq} = \frac{b c^2}{3a^2 + b^2}.$$

Let \mathcal{T}^* denote the family of Poncelet triangles about a circle with center $C = [a_{eq} \cos t, b_{eq} \sin t]$ on \mathcal{E}_{eq} .

Corollary 3. \mathcal{T}^* contains an equilateral triangle.

Let $V^* = [a \cos(t^*), b \sin(t^*)]$ on \mathcal{E} be a vertex of said equilateral.

Proposition 11. t^* is given by the three solutions of:

$$(a^2 + 3b^2) [(3a^2 + b^2) \cos^2 t^* - 2b^2 \sin^2 t - 2b^2 \sin t \sin t^*] \\ + (3a^2 + b^2) [-2a^2 \cos t \cos t^* + (a^2 - 3b^2) \cos^2 t] = 0$$

Proof. It can be shown that a triangular orbit will be equilateral when the triangle $\{V^*, C, [a \cos t, -b \sin t]\}$ is isosceles. \square

Sample loci of X_k , $k = 2, 3, 4, 5$ over \mathcal{T}^* are shown Figure 10 (top). Notice they simultaneously pass through X_1 when the Poncelet triangle becomes an equilateral. In Figure 10 (bottom) are shown the loci of $k = 7, 8, 11, 80$. The first two display the same behavior, while the latter two are stationary.

4.1. C is vertex of X(3). Referring to Figures 11 and 12:

Corollary 4. Over \mathcal{T}^* C is a (major) vertex of \mathcal{L}_3 . If C is interior (resp. exterior) to \mathcal{E}_{eq} , it is interior (resp. exterior) to \mathcal{L}_3 .

Proof. This stems from the fact that the major axis of the X_3 locus passes through C , Proposition 6. \square

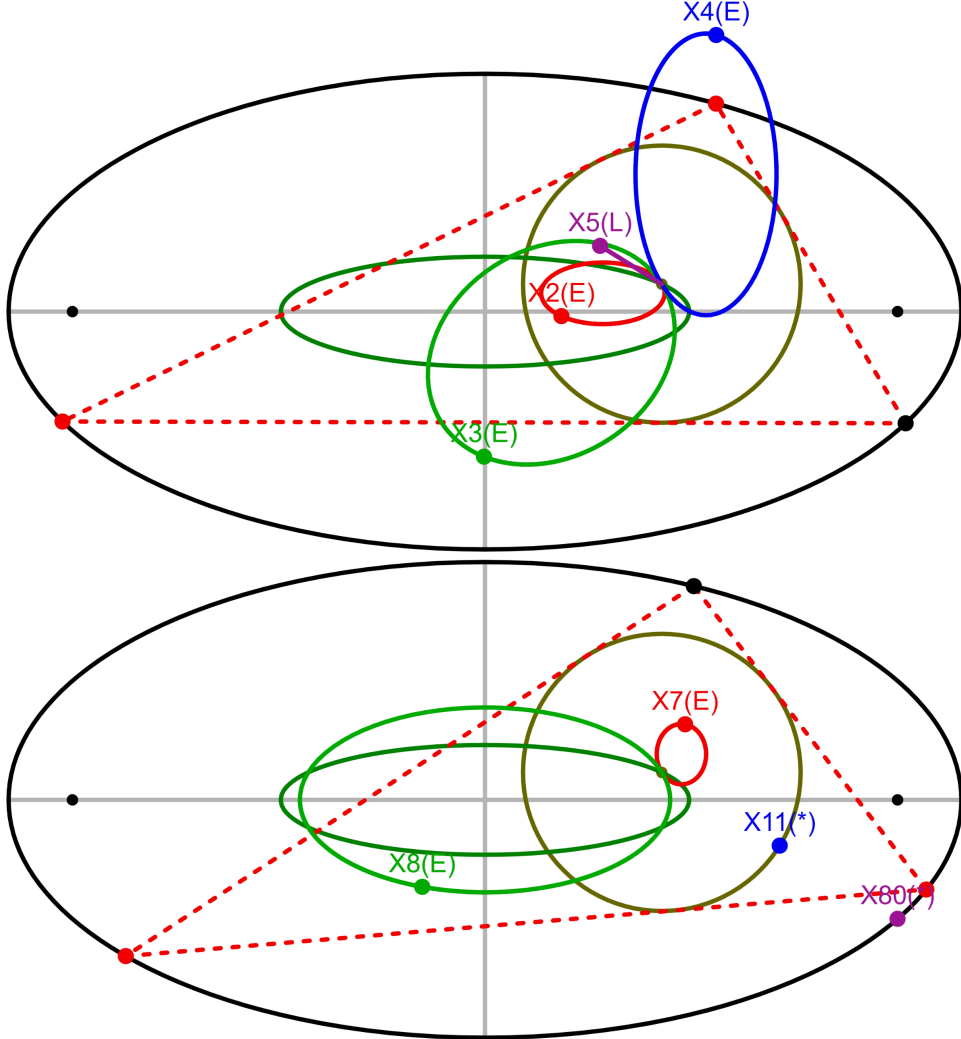


FIGURE 10. **top:** when the incenter is on \mathcal{E}_{eq} (dark green), the loci of X_k , $k = 2, 3, 4, 5$ (red, light green, blue, purple), pass simultaneously through the incenter when the equilateral in the family is traversed, notice that the locus of X_5 (purple) has collapsed to a segment, [live](#); **bottom:** same situation, showing the loci of X_k , $k = 7, 7, 11, 80$ (red, light green, blue, purple). The latter two are stationary on the incircle and \mathcal{E} , respectively, and along the X_1X_5 line, [live](#)

4.2. Invariant aspect ratios: $X(3)$, $X(7)$.

Proposition 12. *Over all C on \mathcal{E}_{eq} the aspect ratio of \mathcal{L}_3 is invariant and given by:*

$$\frac{a_3}{b_3} = \frac{(3a^2 + b^2)(a^2 + 3b^2)(a^4 - b^4)}{c^2(6a^5b + 20a^3b^3 + 6ab^5)}$$

Proof. Evaluating Equation (2) over Proposition 17. \square

Proposition 13. *Over all C on \mathcal{E}_{eq} , the aspect ratio \mathcal{L}_7 is invariant and given by:*

$$\frac{a_7}{b_7} = \frac{2a^2 + b^2}{\sqrt{2a^4 + 5a^2b^2 + 2b^4}}$$

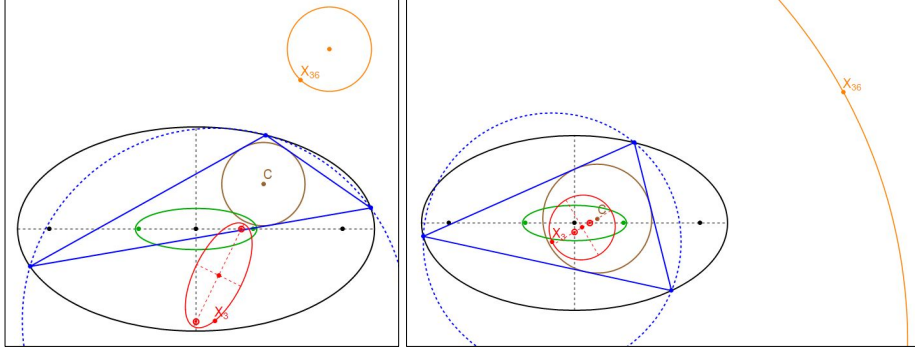


FIGURE 11. On the left (resp. right), $C = X_1$ is outside (resp. inside) \mathcal{E}_{eq} (green). In this case, C is exterior (resp. interior) to the locus of X_3 (red), and the locus of X_{36} (orange) is disjoint with (resp. contains) \mathcal{E} .

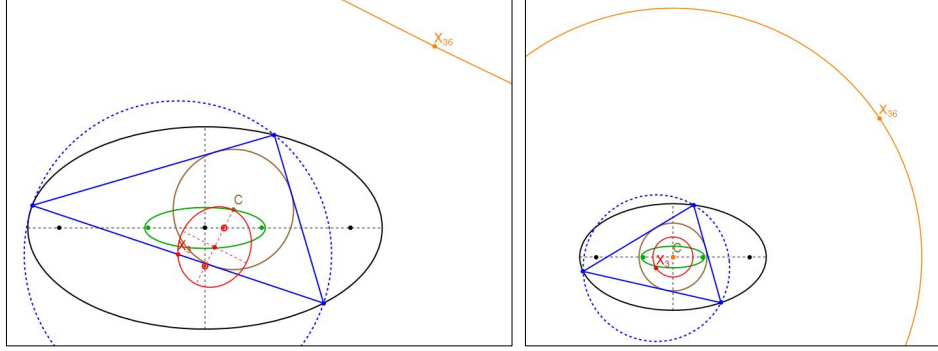


FIGURE 12. On the left (resp. right), $C = X_1$ is on (resp. at the center of) \mathcal{E}_{eq} (green). In this case, C is a vertex (at the center) of the locus of X_3 (red), and the locus of X_{36} (orange) is a line (resp. a circle concentric with \mathcal{E}).

Proof. Direct from Proposition 5. □

4.3. Segment $X(5)$.

Proposition 14. *Over all $C = [a_{eq} \cos t, b_{eq} \sin t]$ on \mathcal{E}_{eq} , \mathcal{L}_5 is a segment ($b_5 = 0$) of length l_5 with an endpoint on C and the other at $F'_{5,eq}$. These are given by:*

$$l_5^2 = \frac{c^8 (a^6 + 15a^4b^2 + 15a^2b^4 + b^6 - c^6 \cos(2t))}{16 (3a^5b + 10a^3b^3 + 3ab^5)^2}$$

$$F'_{5,eq} = \left[\frac{(a^4 - b^4) \cos t}{2(a^3 + 3ab^2)}, \frac{(a^4 - b^4) \sin t}{2(3a^2b + b^3)} \right]$$

Proof. Applying Proposition 7 on Proposition 17. □

Corollary 5. *Over \mathcal{T}^* the locus of X_{12} (internal center of similitude of the incircle and the Euler circle [18]), is a segment with one endpoint at C .*

Proof. This must be the case because the segment locus of the Euler center X_5 passes through C . □

4.4. **Stationary X(11), X(80).** Referring to Figure 19:

Proposition 15. Over \mathcal{T}^* , the Feuerbach point X_{11} (resp. X_{80} , the reflection of X_1 on X_{11}) is stationary at the non- C intersection of the segment-locus of X_5 with the incircle (resp. with \mathcal{E}). With $C = [a_{eq} \cos t, b_{eq} \sin t]$ on \mathcal{E}_{eq} , these are given by:

$$X_{11}^* = \frac{a^2 + b^2}{c^2} [a_{eq} \cos t, -b_{eq} \sin t]$$

$$X_{80}^* = [a \cos t, -b \sin t]$$

Note that $X_k, k = 1, 5, 11, 12, 80, \dots$, are points on the X_1X_5 line [19].

Proof. CAS manipulation. \square

Observation 3. Over \mathcal{T}^* , the locus of X_{106} (isog. conj. of X_1X_2 with the line at infinity) is a circle passing through X_{80} .

Lemma 1. Let $C = [a_{eq} \cos t, b_{eq} \sin t]$. Over \mathcal{T}^* , the intersection $I^* = [x^*, y^*]$ of the ray X_1X_5 with \mathcal{E} is given by:

$$x^* = \frac{(a^2 v (a^4 - 3a^2 b^2 - 2b^4) \sin^2 t - b^4 u^2 \cos^2 t) a \cos t}{b^4 u^2 \cos^2 t + a^4 v^2 \sin^2 t}$$

$$y^* = \frac{(b^2 u (2a^4 + 3a^2 b^2 - b^4) \cos^2 t + a^4 v^2 \sin^2 t) b \sin t}{b^4 u^2 \cos^2 t + a^4 v^2 \sin^2 t}$$

where $u = (3a^2 + b^2)$ and $v = (3b^2 + a^2)$.

Referring to Figure 13:

Proposition 16. In \mathcal{T}^* , the Poncelet triangle $I^*B_1B_2$ is an isosceles, unique in the family (other than the equilateral), with base B_1B_2 , the chord of E tangent to the incircle at the stationary X_{11} .

Proof. The triangle is an isosceles since I^*, X_1, X_5 are collinear. The base must be tangent to the incircle (via Poncelet) at X_{11} , since the latter is collinear with X_1 and X_5 [18]. We omit the expressions for B_1 and B_2 since they are rather long. \square

4.5. **Line X(36).** In Proposition 9 we saw that over \mathcal{T} , the locus X_{36} was a circle. Nevertheless, and referring to Figure 12 (left):

Proposition 17. Over \mathcal{T}^* , with $C = [x_c, y_c]$ on \mathcal{E}_{eq} , the locus of X_{36} degenerates to the line:

$$b^2 x_c x + a^2 y_c y = \frac{b^2 (a^4 + 2a^2 b^2 + 5b^4) x_c^2 + a^2 (5a^4 + 2a^2 b^2 + b^4) y_c^2}{c^4}$$

Proof. Direct from Proposition 9, taking the limit when (x_c, y_c) is on \mathcal{E}_{eq} and simplifying. \square

Referring to Figure 11:

Observation 4. Over \mathcal{T}^* , the locus of X_{36} is disjoint with (resp. contains) \mathcal{E} if C is exterior (resp. interior) to \mathcal{E}_{eq} .

Referring to Figure 14:

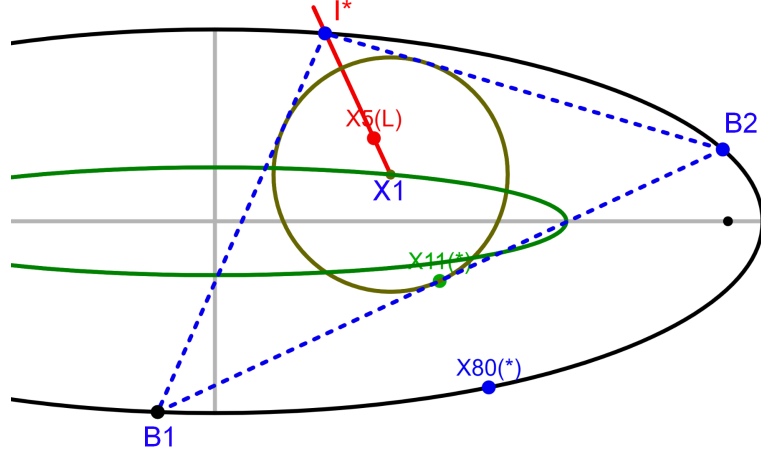


FIGURE 13. Construction for Proposition 16: $C = X_1$ on \mathcal{E}_{eq} , the Poncelet triangle has a vertex on the intersection I^* of the ray X_1X_5 with \mathcal{E} . The said triangle is an isosceles, and its base B_1B_2 is the chord of \mathcal{E} touching the incircle at X_{11} . [live](#)

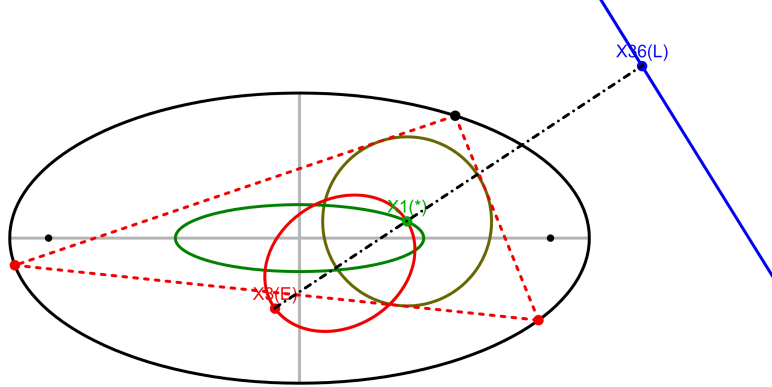


FIGURE 14. When X_3 is on the non- X_1 major vertex of its locus (red), X_3X_1 is perpendicular to the line-locus of X_{36} . At this moment, $|X_1X_{36}|$ is minimal. [live](#)

Proposition 18. *If $C = [x_c, y_c]$ is on \mathcal{E}_{eq} , the major axis of \mathcal{L}_3 is perpendicular to the line locus of X_{36} . These meet at:*

$$X_{36}^\perp = c^{-4} [x_c(a^4 + 2a^2b^2 + 5b^4), y_c(b^4 + 2b^2a^2 + 5a^4)]$$

Proof. Direct from Proposition 6 which the X_3 -locus major axis, and Proposition 17. \square

Observation 5. *Over \mathcal{T}^* , when X_3 passes through $C = X_1$, i.e., the major vertex of its locus, X_{36} is on the line at infinity.*

Referring to Figure 15, we specialize Proposition 10 to its degenerate form:

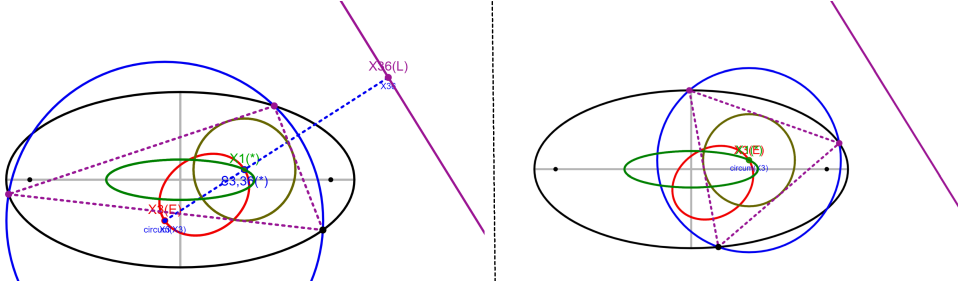


FIGURE 15. **left:** When X_3 is on the non- X_1 vertex of its locus, the circumradius R is maximized and $|X_1X_{36}|$ is minimal; **right:** if X_3 on X_1 , the triangle is equilateral, R is minimized while $|X_1X_{36}|$ is ‘maximal’, since X_{36} is on the line at infinity. [live](#)

Proposition 19. Over \mathcal{T}^* , when X_3 is on the non- X_1 major vertex of its locus, the distance $|X_1X_{36}|$ is minimal and given by:

$$|X_1X_{36}|_{\min} = \frac{4(a^2 + b^2) \sqrt{a^4 y_c^2 + b^4 x_c^2}}{c^4}$$

Furthermore, the circumradius R is minimized (resp. maximized) when $X_3 = X_1$ (resp. X_3 is on the non- X_1 vertex of its locus).

$$R_{\min} = 2 \left(\frac{b\sqrt{a^4 - c^2 x_c^2} - a\sqrt{b^4 + c^2 y_c^2}}{c^2} \right)$$

$$R_{\max} = \frac{(a^2 + b^2) \sqrt{a^4 + 6a^2 b^2 + b^4} \sqrt{a^4 y_c^2 + b^4 x_c^2}}{2a^2 b^2 c^2}$$

Referring to Figure 16:

Observation 6. Over all C on \mathcal{E}_{eq} , the envelope of the line locus of X_{36} is an oval of degree 6.

4.6. Elliptic $X(59)$. Referring to Figure 17, in several Poncelet families studied, the locus of X_{59} , the isogonal conjugate of X_{11} , is either an oval or a self-intersected curve, e.g., see [11, Fig.2] and [26, Fig.9].

Nevertheless, it collapses to a conic in the following two cases. Firstly:

Proposition 20. In Chapple’s porism, the locus of X_{59} is an ellipse with major axis on X_1X_3 , with semi-axis lengths given by:

$$a_{59, \text{chapple}} = R, \quad b_{59, \text{chapple}} = \frac{R\sqrt{R^2 - d^2}}{\sqrt{9R^2 - d^2}}$$

The isogonal conjugate $g(P)$ of a point P with respect to a triangle T is the point of concurrence of the cevians of P reflected upon the angle bisectors [36]. In [33] it is shown that the locus of $g(P)$ over circle-inscribed Poncelet triangles is a circle. As above, let \mathcal{T}_g be a family of Poncelet triangles interscribed between two generic conics $\mathcal{E}, \mathcal{E}_c$. Referring to Figure 18, the following is proved in [10]:

Lemma 2. Over \mathcal{T}_g , the locus of $g(P)$ is a conic. If P is on \mathcal{E}_c the locus is an ellipse interior to \mathcal{E} and touching it at a point.

Secondly, referring to Figure 17 (bottom right) and Figure 19:

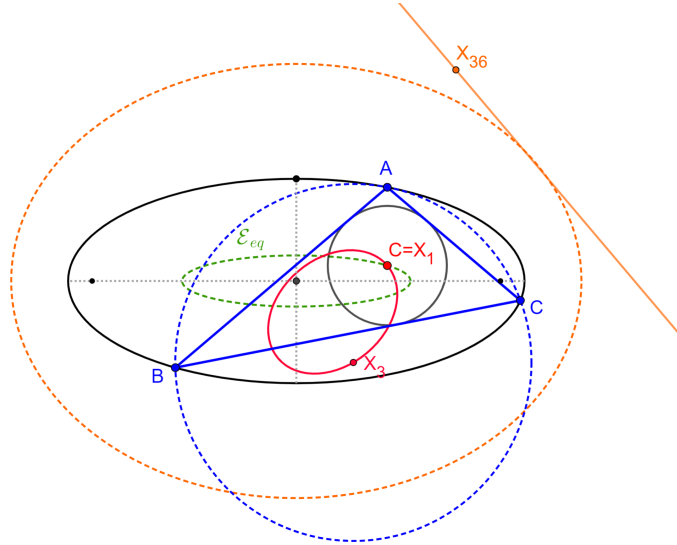


FIGURE 16. Over all $C = X_1$ on \mathcal{E}_{eq} (dashed green), the envelope of the line locus of X_{36} is an oval of degree 6 (dashed orange).

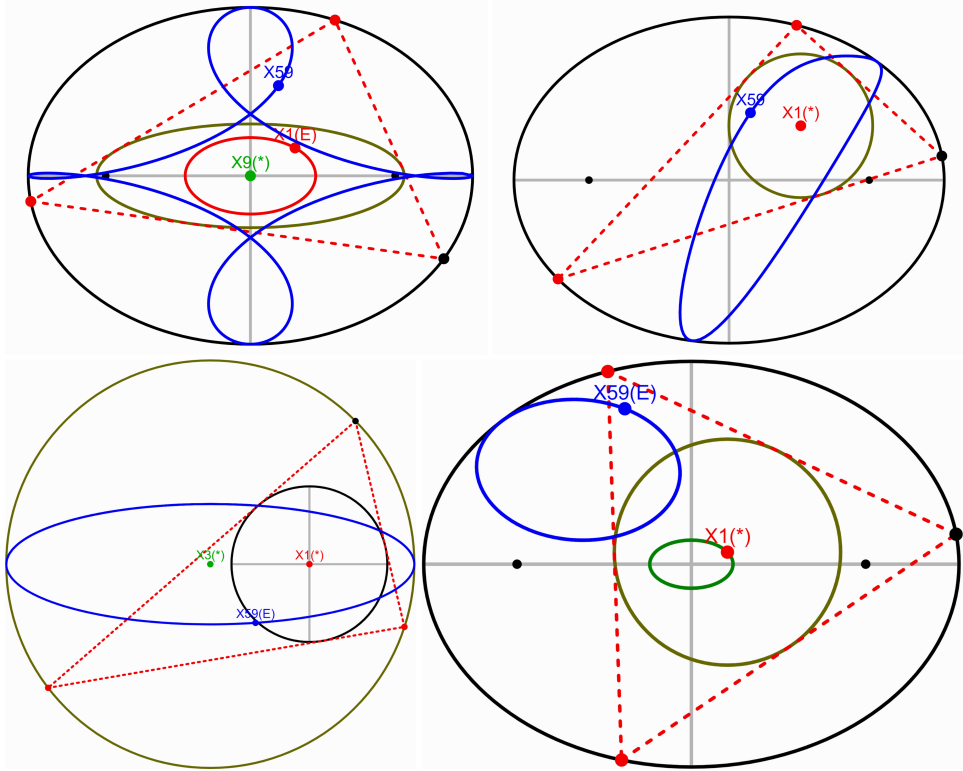


FIGURE 17. The locus of X_{59} (isogonal conjugate of X_1 in (i) the confocal pair (top left), (ii) a generic incircle porism (top right), (iii) Chapple's porism, where it is an ellipse (top bottom), and (iv) an incircle porism with X_1 on \mathcal{E}_{eq} (dark green), notice X_{59} is a conic, tilted with respect to \mathcal{E} , which it touches at a single point.

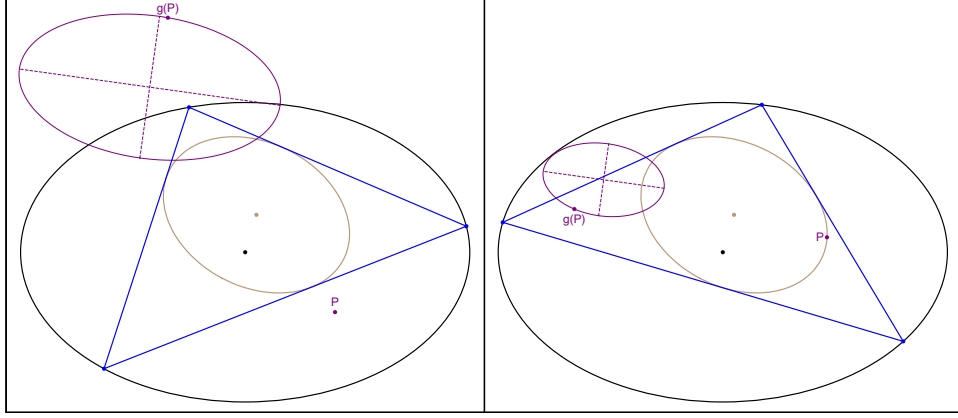


FIGURE 18. Results from [10]: **left**: over generic Poncelet triangles, the locus of the isogonal conjugate $g(P)$ of a fixed point P is a conic (purple); **right**: if P is on the caustic, the locus of $g(P)$ is an ellipse that touches \mathcal{E} at one point.

Corollary 6. *Over \mathcal{T}^* , the locus of X_{59} is an ellipse interior to \mathcal{E} and touching it at a point.*

Proof. X_{59} is the isogonal conjugate of X_{11} [18], which is stationary on the incircle over \mathcal{T}^* . \square

Furthermore, let I^* denote the touch-point between the elliptic locus of X_{59} (over \mathcal{T}^*) and \mathcal{E} .

Observation 7. *When the Poncelet triangle is an isosceles, i.e., one of its vertices is I^* , X_{59} is at I^* . When the Poncelet triangle is an equilateral, X_{59} ‘blows up’ at a major vertex of its locus.*

5. ENVELOPES

As before, let \mathcal{T} be a family of Poncelet triangles inscribed in an ellipse \mathcal{E} and circumscribing a circle \mathcal{K} with center $C = X_1$.

5.1. Circumcircle. Referring to Figure 20:

Proposition 21. *Over \mathcal{T} , the envelope of the circumcircle are two nested circles, each tangent to \mathcal{E} at two points and centered at the foci F_3 and F'_3 of X_3 locus (Proposition 6).*

Proof. Let $C = (x_c, y_c)$ be the center of caustic and r the radius of the caustic given by Proposition 2; the incircle \mathcal{K} is then given by $(x - x_c)^2 + (y - y_c)^2 = r^2$. Let $\lambda = \cos u + i \sin u$ in the symmetric parametrization of Section 2.2, obtain the circumcircle \mathcal{K}' :

$$\begin{aligned} \mathcal{K}'(x, y) = x^2 + y^2 - & \left(\frac{(a^3 b - \delta) \cos u}{b a^2} + \frac{c^2 y_c x_c \sin u}{b a^2} + \frac{c^2 x_c}{a^2} \right) x \\ & + \left(-\frac{c^2 x_c y_c \cos u}{a b^2} + \frac{c^2 y_c}{b^2} + \frac{(a b^3 - \delta) \sin u}{a b^2} \right) y + \frac{c^2 x_c \cos u}{a} + \frac{c^2 y_c \sin u}{b} - \frac{\delta}{b a} = 0 \end{aligned}$$

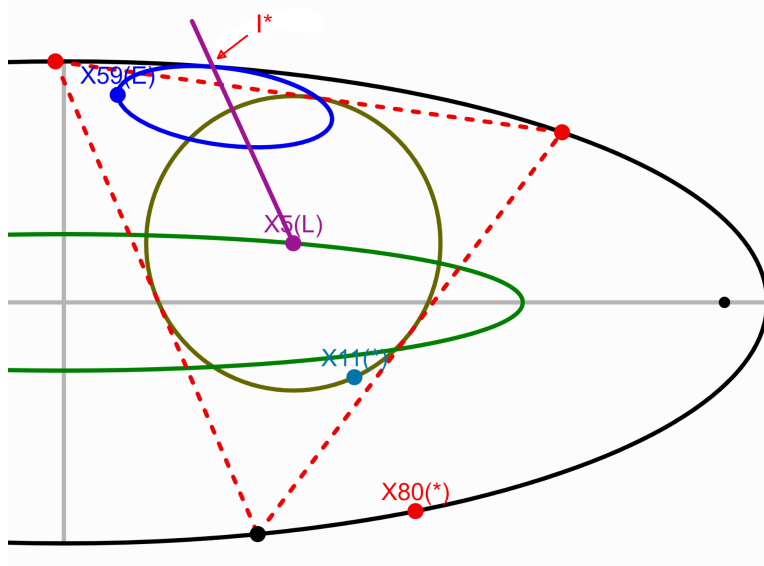


FIGURE 19. When the incenter is on \mathcal{E}_{eq} (dark green), the locus of X_5 is a line, and X_{11} and X_{80} are stationary on the incircle and \mathcal{E} , respectively. The locus of X_{59} is an ellipse (blue), internally-tangent to \mathcal{E} at I^* (see Lemma 1). In the picture, X_5 is on X_1 , i.e., the Poncelet triangle is an instantaneous equilateral. When this happens, X_{59} is at a vertex of its locus. [live](#)

The envelope of this family of circles is obtained by setting:

$$\mathcal{K}'(x, y) = 0, (\partial \mathcal{K}' / \partial u)(x, y) = 0$$

With the above equations this yields the union of two circles $\mathcal{K}_1 = (O_1, r_1)$ and $\mathcal{K}_2 = (O_2, r_2)$ where:

$$\begin{aligned} O_1 &= [0, -y_c c^2 / b^2] = [0, y_c (1 - (a/b)^2)] = F'_3 \\ r_1 &= (a/b^2) \sqrt{b^4 + c^2 y_c^2} \\ O_2 &= [x_c c^2 / a^2, 0] = [x_c (1 - (b/a)^2), 0] = F_3 \\ r_2 &= (b/a^2) \sqrt{a^4 - c^2 x_c^2} \end{aligned}$$

\mathcal{K}_1 touches \mathcal{E} at $[\pm(a/b)\sqrt{b^2 - y_c^2}, y_c]$; \mathcal{K}_2 touches \mathcal{E} at $[x_c, \pm(b/a)\sqrt{a^2 - x_c^2}]$. \square

Given two fixed nested (resp. unnested) circles, the locus of the center of circles simultaneously tangent to them is a conic with foci on their centers and with major axis length equal to the difference (resp. sum) of their radii [22, thm.14, p.57]. In our case, the circumcircles of a Poncelet family circumscribing a circle are tangent to the two circular boundaries of their envelope. In Equation (2), an expression is derived for a_3 , the semi-axis length of the locus of X_3 . It follows that:

Corollary 7. $|r_1 - r_2| = 2a_3$.

For the general case, experimental evidence suggests:

Conjecture 1. *Over \mathcal{T}_g , either component of the envelope of the circumcircle is a conic if and only if \mathcal{E}_c is a circle, in which case both components are circles (Proposition 21).*

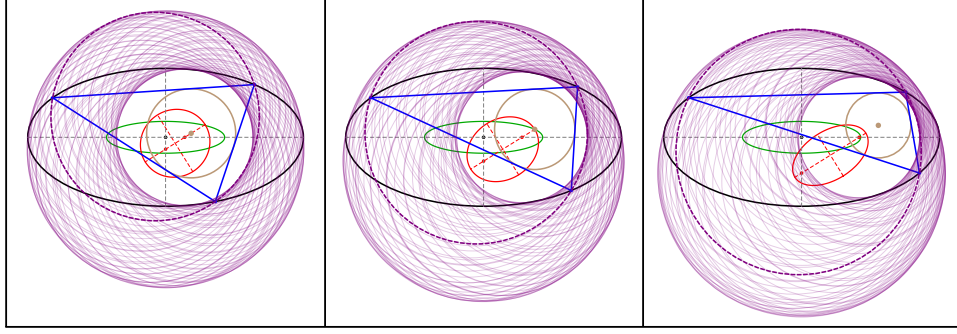


FIGURE 20. The envelope of the circumcircle consists of two nested circles twice tangent to \mathcal{E} and centered on the foci of the X_3 locus (red). Left, middle, right show three positions for $C = X_1$: interior, on the boundary, and exterior to \mathcal{E}_{eq} (green), respectively. [Video](#)

Note that if the outer conic is a circle, said envelope is not defined.

5.2. Radical axis. Let \mathcal{R} denote the radical axis of incircle and circumcircle of a triangle, i.e., the line whose points have equal circle power with respect to the two said circles [36]. X_1X_3 must be perpendicular to \mathcal{R} since it is the line that passes through both circle centers. According to [18], X_{3660} is the ‘trace’ of \mathcal{R} , i.e., the perpendicular intersection of X_1X_3 with the radical axis.

Referring to Figure 21:

Proposition 22. *Over \mathcal{T} , the envelope of \mathcal{R} is a conic whose major axis coincides with that of the X_3 locus (see Proposition 6). It will be an ellipse (resp. hyperbola) if C is interior (resp. exterior) to \mathcal{E}_{eq} .*

Proof. Let $C = (x_c, y_c)$ be the center of caustic and r the radius of the caustic given by Proposition 2; the incircle \mathcal{K} is then given by $(x - x_c)^2 + (y - y_c)^2 = r^2$. Let $\lambda = \cos u + i \sin u$ in the symmetric parametrization of Section 2.2, obtain the circumcircle \mathcal{K}' :

$$\begin{aligned} \mathcal{K}'(x, y) = x^2 + y^2 - & \left(\frac{(a^3b - \delta)}{ba^2} \cos u + \frac{c^2y_c x_c}{ba^2} \sin u + \frac{c^2x_c}{a^2} \right) x \\ & + \left(-\frac{c^2x_c y_c}{a b^2} \cos u + \frac{(a b^3 - \delta)}{a b^2} \sin u + \frac{c^2y_c}{b^2} \right) y + \frac{c^2x_c}{a} \cos u + \frac{c^2y_c}{b} \sin u - \frac{\delta}{ba} = 0 \end{aligned}$$

The radical axis of $(\mathcal{K}, \mathcal{K}')$, is given by $l(u)x + m(u)y + n(u) = 0$, with:

$$\begin{aligned} l(u) &= c^4 (-bx_c y_c c^2 \sin u + b(\delta - a^3b) \cos u + b^2(a^2 + b^2)x_c) \\ m(u) &= c^4 (a(a b^3 - \delta) \sin u - ax_c y_c c^2 \cos u + a^2(a^2 + b^2)y_c) \\ n(u) &= a^2 b y_c c^6 \sin u + a b^2 x_c c^6 \cos u + a^2 b^2 c^2 (-a^2 x_c^2 + b^2 y_c^2) + a^4 b^4 (a^2 + b^2) \\ &\quad - ab(a^4 + b^4)\delta. \end{aligned}$$

The envelope of the family of lines above is given by:

$$E(u) = \left[\frac{n'(u)m(u) - m'(u)n(u)}{m'(u)l(u) - l'(u)m(u)}, -\frac{n'(u)l(u) - l'(u)n(u)}{m'(u)l(u) - l'(u)m(u)} \right]$$

Developing the calculations it follows that the envelope is parametrized by:

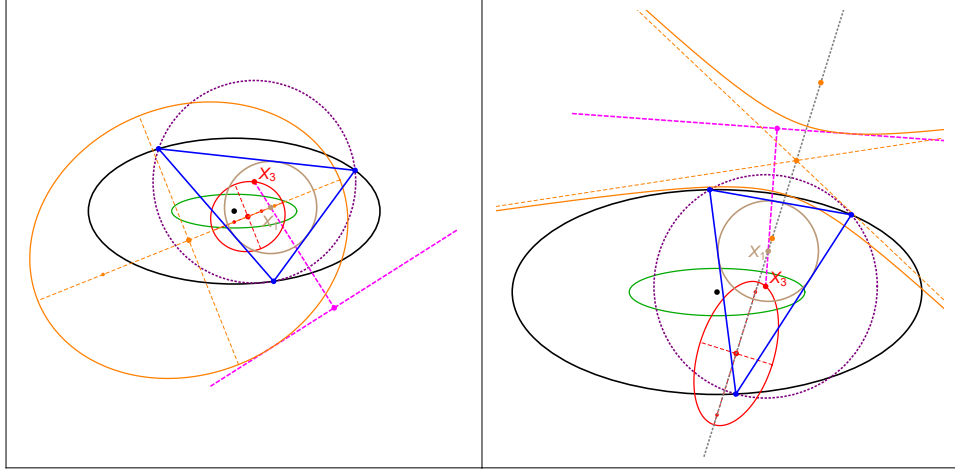


FIGURE 21. Left (resp. right): envelope (orange) of \mathcal{R} (dashed magenta) is an ellipse (resp. hyperbola), when $C = X_1$ is interior (resp. exterior) to \mathcal{E}_{eq} (green ellipse). The major axis of the locus of X_3 (red) coincides with that of the envelopes.

$$E(u) = \left[\frac{k_1 \sin u + k_2 \cos u + k_3}{d_1 \sin u + d_2 \cos u + d_3}, \frac{m_1 \sin u + m_2 \cos u + m_3}{d_1 \sin u + d_2 \cos u + d_3} \right]$$

Here all constants are long expressions involving the variables (a, b, c, x_c, y_c) . Eliminating the variables we obtain that the envelope is given implicitly by a quadratic equation and so it is a conic.

to do. □

Referring to Figure 22:

Corollary 8. *Over \mathcal{T} , the envelope of \mathcal{R} is a parabola if C is on the boundary of \mathcal{E}_{eq} whose axis of symmetry is the major axis of the X_3 locus, i.e., its directrix is parallel to the line-locus of X_{36} (Proposition 17).*

Proof. When the family is at the equilateral position, X_1 and X_3 coincide, and \mathcal{R} is the line at infinity. □

Based on experimental evidence:

Conjecture 2. *Over \mathcal{T} , the envelope of \mathcal{R} is a conic if and only if the Poncelet caustic is a circle.*

The Feuerbach point X_{11} is where incircle and nine-point circle touch. Therefore, the radical axis of said circles is tangent to the incircle at X_{11} . Let said axis be called $L(101)$ after [36]. Therefore:

Corollary 9. *Over \mathcal{T} , the envelope of $L(101)$ is the incircle itself. If C is on \mathcal{E}_{eq} , X_{11} is stationary (Proposition 15), therefore, in such a case said envelope is undefined.*

The *orthic axis*, called \mathcal{L}_3 in [36] (resp. *anti-orthic axis*, \mathcal{L}_1) is the radical axis of the circumcircle and the nine-point (resp. Bevan) circle [36, Radical line], the latter is centered on X_5 (resp. X_{40}) and has radius $R/2$ (resp. $2R$). Experimentation shows:

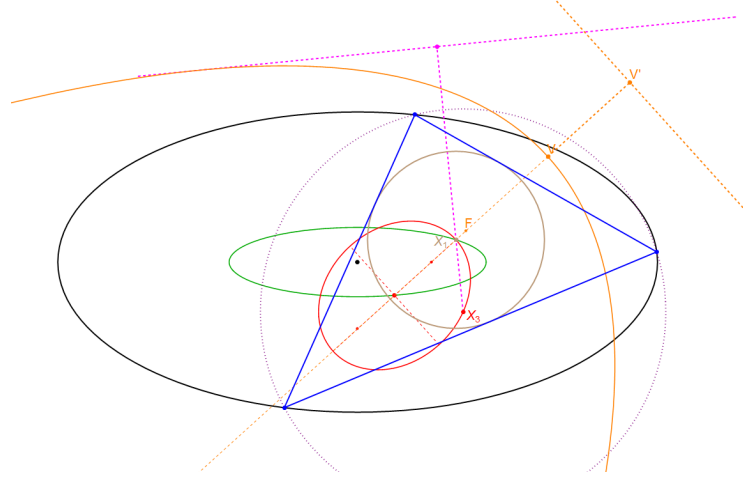


FIGURE 22. When $C = X_1$ is on the boundary of \mathcal{E}_{eq} (green ellipse), the envelope of \mathcal{R} (dashed magenta) is parabolic (orange, focus F , vertex V); the axis of symmetry (dashed orange) is the major axis of the locus of X_3 (red). Also shown is the directrix of the parabola (dashed orange), with V' its intersection with the axis of symmetry.

Observation 8. Over \mathcal{T} , the envelope of both \mathcal{L}_3 and \mathcal{L}_1 are conics: an (ellipse, parabola, hyperbola) if C is (interior, on the boundary, exterior) to E_{eq} respectively. Nevertheless, the envelope axes and those of the X_3 locus are not axis-aligned.

6. ELLIPTICITY OF $X(k)$, $k=1, 7, 8$

In [11, 29] it is proved that the locus of the incenter X_1 is a conic if the Poncelet ellipse pair is confocal (elliptic billiard). In [16, Conj.3] it is conjectured that X_1 sweeps a conic if and only if the pair is confocal, and a proof is still outstanding.

Experiments with ten different Poncelet families (see six of them in Figures 23 and 24) are summarized in Table 1. In turn, these suggest:

Conjecture 3. The locus of X_7 and/or X_8 are conics if and only if (i) the Poncelet conic pair is confocal or (ii) the caustic is a circle (in which case X_1 is stationary).

Note that for the case of the bicentric pair, the locus of both X_7 and X_8 are circles [21].

7. FOUR SPECIAL FAMILIES

We study four special families of ellipse-inscribed Poncelet triangles about the incircle. Referring to Figure 25, these are: (i) focal- X_1 : the caustic is centered on a focus of E ; (ii) iso- X_2 : caustic is on a first special point such that the barycenter X_2 is stationary; (iii) focal- X_4 : caustic is centered on a second special point such that the orthocenter X_4 is stationary on a focus of E ; (iv) iso- X_7 : caustic is centered on a third special point such that the Gergonne point X_7 is stationary.

In the calculations below, R , r , l_i , $i = 1, 2, 3$ refer to a triangle's circumradius, inradius, and sidelengths, respectively.

7.1. Focal-X(1). Referring to Figure 25 (top left):

Family	Outer	Inner	X_1	X_7	X_8	bit.ly/<code>
Confocal	E	E	E	E	E	46KYk4D
Chapple	C	C	P	C	C	4cqyGmN
Incircle	E	C	P	E	E	3M50bHG
Circ-caustic	E	C	P	E	E	4fK8Exy
Homothetic	E	E	-	-	-	3M4sG8G
Dual	E	E	-	-	-	3WHkQqg
Conf. Excentrals	E	E	-	-	-	3WGARgk
Inellipse	C	E	-	-	-	4fKZPUv
Brocard	C	E	-	-	-	4fKQmMH
MacBeath	C	E	-	-	-	3M3xtaj

TABLE 1. The loci of X_k , $k = 1, 7, 8$ for 10 Poncelet conic configurations. ‘Inner’ and ‘Outer’ indicate if such conics are either ellipses (E) or circles (C). Under columns labeled X_k ($k = 1, 7, 8$), symbols ‘E’, ‘C’, ‘P’, ‘-’ indicate if the corresponding locus is an ellipse, a circle, a point, or a non-conic, respectively. The pattern that emerges is that X_7 and X_8 can only be conics if ‘Inner’ is a circle, in which case X_1 is a point. The confocal family is one exception: the inner conic is a (confocal) ellipse, and all three centers sweep conics. Note: the last column gives a hyperlink to an animated view of the family.

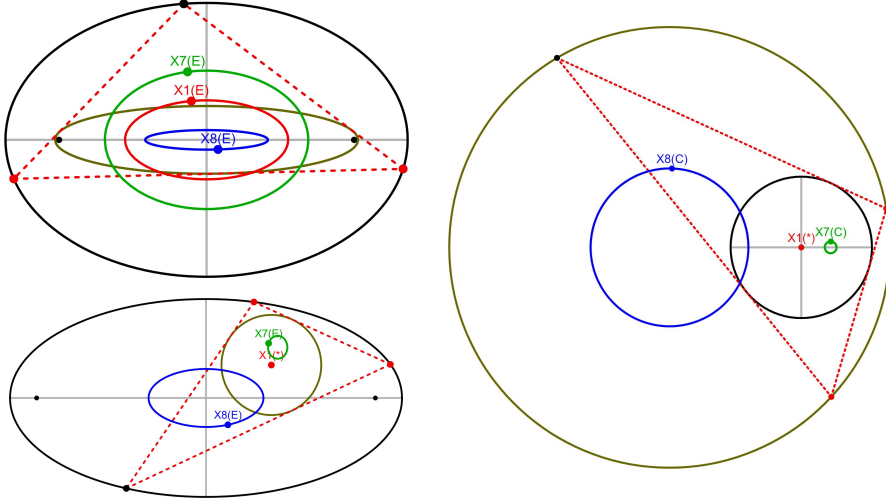


FIGURE 23. Three Poncelet families for which the loci of X_k , $k = 1, 7, 8$ are conics: (i) top left: confocal pair; bottom left: generic circular caustic; (iii) right: Chapple's porism (bicentric $n = 3$). Note that in (ii) and (iii), X_1 is stationary (center of caustic). Also note that in (iii), the loci of X_7 and X_8 are circles.

Proposition 23. *The caustic centered at $C_1 = [c, 0]$ closes Poncelet $N = 3$ with radius r_1 given by:*

$$r_1 = \frac{b^2}{c^2} \left(\sqrt{a^2 + c^2} - a \right)$$

Proof. Direct from Proposition 2. □

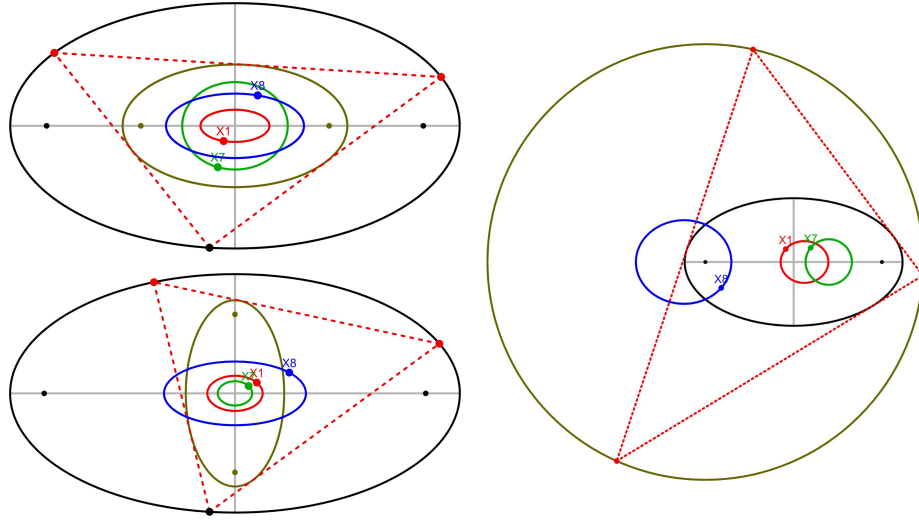


FIGURE 24. Three Poncelet families for which the loci of X_k , $k = 1, 7, 8$ are non-conics: (i) top left: pair of homothetic ellipses; bottom left: pair of 'dual' ellipses; (iii) right: the MacBeath family.

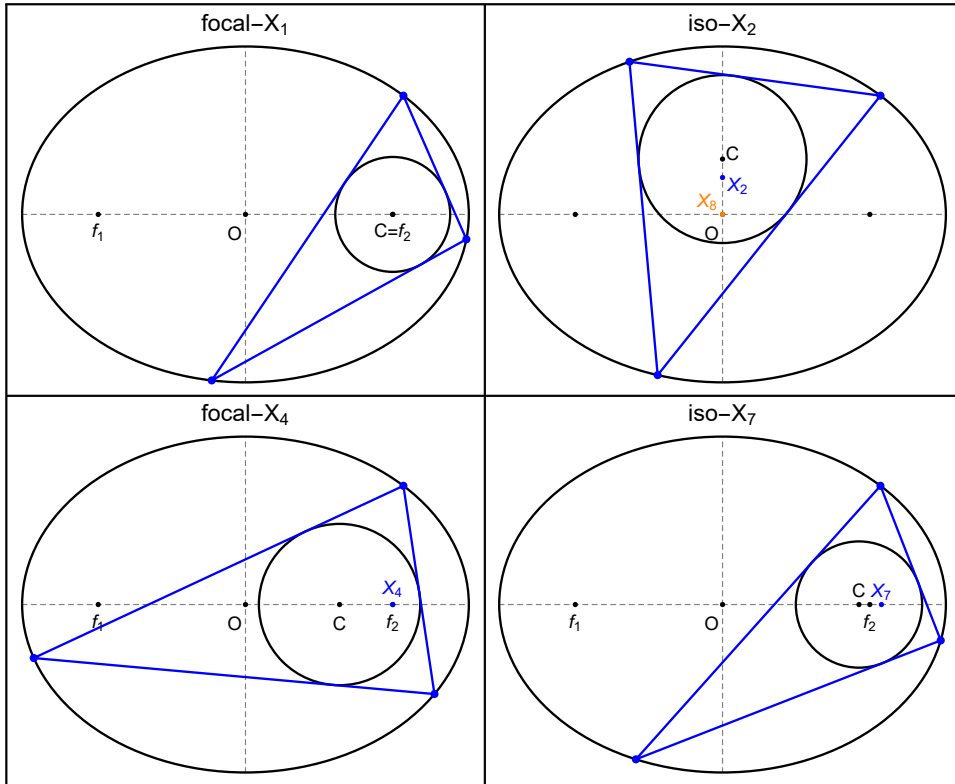


FIGURE 25. Four families of ellipse-inscribed Poncelet triangles about the incircle: focal- X_1 (top left); iso- X_2 (top right); focal- X_4 (bottom left); iso- X_7 (bottom right). [Video](#)

Observation 9. *The focal- X_1 family is the polar image of the vertices of Chapple's Porism (a porism of triangles interscribed between two circles [21]), with respect to the circumcircle, i.e., it is its tangential triangle. The former's X_1 coincides with the latter's circumcenter X_3 .*

While bicentric n -gons (a generalization of Chapple's porism) conserve the sum of cosines [28], their polar family conserve $\sum_{i=1}^n \sin(\theta_i/2)$, for all $n \geq 3$ [2, prop.26].

Proposition 24. *For the focal- X_1 family, the invariant sum of half-angle sines is given by:*

$$\sum_{i=1}^3 \sin \frac{\theta_i}{2} = \frac{c^2 - a^2 + a\sqrt{a^2 + c^2}}{c^2}$$

7.2. **Iso- $\mathbf{X}(2)$.** Referring to Figure 25 (top right):

Proposition 25. *For a circular caustic with center and radius given by:*

$$C_2 = \left[0, \frac{cb}{2a} \right], \quad r_2 = \frac{b}{2}$$

The barycenter X_2 is stationary at

$$\left[0, \frac{cb}{3a} \right]$$

Corollary 10. *Over iso- X_2 triangles, the Nagel point X_8 is stationary at E 's center.*

Proof. Direct from the location of the stationary barycenter and the fact that $|X_1X_8| = 3|X_1X_2|$ [36, Incenter, eqn.(11)]. In fact, $|X_1X_8| = 3(cb/(2a) - cb/(3a)) = cb/(2a) = |C_2|$. \square

Corollary 11. *The Spieker center X_{10} , incenter of the medial triangle and the midpoint of X_1 and X_8 [18] will be stationary on E 's minor axis.*

Observation 10. *Since X_2 is stationary, the family conserves $|X_1X_2|$, which for any triangle with sidelengths l_i is given by [36, Triangle Centroid, eqn.(11)]:*

$$|X_1 - X_2|^2 = -\frac{\sum l_i^3 + 9 \prod l_i - 2(l_2 l_1^2 + l_3 l_1^2 + l_2^2 l_1 + l_3^2 l_1 + l_2 l_3^2 + l_2^2 l_3)}{9 \sum l_i}$$

Lemma 3. *The barycenter X_2 of the MacBeath is stationary.*

Proof. The foci of the caustic are X_3 and X_4 , therefore X_2 must be fixed, $|X_3X_2| = |X_3X_4|/3$ [36, Triangle Centroid, eqn. (13)]. Consider also that MacBeath family are the intouch triangles of bicentric polygons (Chapple's porism). The X_2 of the intouch triangle is the Weill point X_{354} of the reference [18], shown to be stationary over the bicentric family [21, Thm. 4.1]. \square

Proposition 26. *Given an outer ellipse E centered on O and a point C in its interior, there is an (elliptic) caustic K centered on C such that over Poncelet, X_2 on OC is stationary.*

Referring to Figure 26:

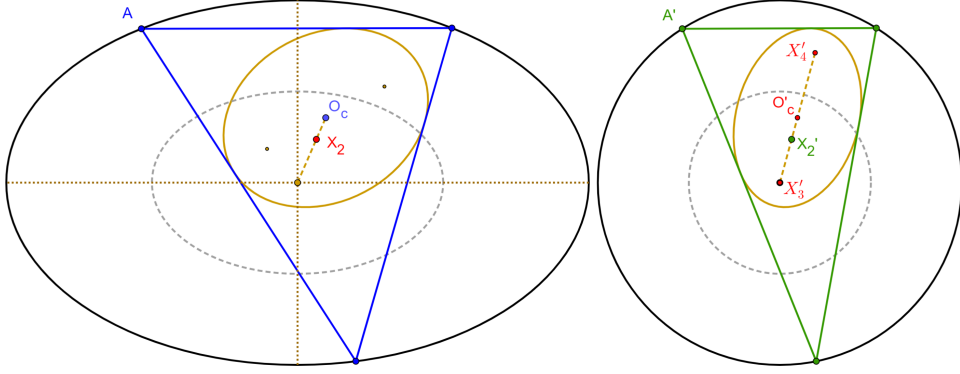


FIGURE 26. **left:** To find a caustic at a given center O_c that keeps X_2 stationary, find an affinity that sends the outer ellipse E' to a circle E' ; **right:** in such an affine projection find the MacBeath caustic with a focus at the center and another at the reflection of the latter about the projection of O_c under the affinity. The desired caustic on the left system is the image of said MacBeath caustic under the inverse affinity. Because affinities preserve collinearities, the stationary X_2 will lie on OO_c , [Video](#)

Proof. Let \mathcal{A} be an affine transform that sends E to a circle E' . Let K' be the unique MacBeath caustic in E' with a first focus at its center and the other the reflection of E' about $C' = \mathcal{A} \cdot C$. Recall that conic centers are equivariant with respect to affinities. Let K be the image of K' under \mathcal{A}^{-1} . The X_2 of the family in (E, K) will be stationary because (i) the MacBeath's centroid is stationary, [Lemma 3](#) and (ii) the centroid is the only triangle center which is equivariant with respect to affinities [18]. X_2 must lie on OC because affinities preserve collinearities. Notice it will nevertheless not lie on the major axis of K (foci are not equivariant). \square

7.3. Focal-X(4). Referring to [Figure 25](#) (bottom left):

Proposition 27. *The orthocenter X_4 is stationary at a focus $f = [\pm c, 0]$ of E for the circular caustic with center and radius given by:*

$$C_4 = \left[\pm \frac{a^2 c}{2a^2 - c^2}, 0 \right], \quad r_4 = \frac{a(a^2 - c^2)}{2a^2 - c^2}$$

Numeric search over the first forty-thousand triangle centers on [18] reveals:

Referring to [Figure 27](#):

Observation 11. *For the focal- X_4 family the center (resp. other focus) of E is X_{7952} (resp. X_{18283}) on [18]. The locus of the circumcenter X_3 is an ellipse with a focus at E 's center. The locus of X_{20} is twice as large, with a focus on E 's distal focus.*

Definition 1. A triangle's *polar circle* is centered on X_4 and has squared radius given by [36, Polar Circle]:

$$r_{pol}^2 = 4R^2 - \frac{\sum l_i^2}{2}$$

This quantity is positive (resp. negative) for obtuse (resp. acute triangles).

Proposition 28. *The focal- X_4 family conserves the (negative) squared radius of its polar circle at $r_{pol}^2 = -b^4/(a^2 + b^2)$.*

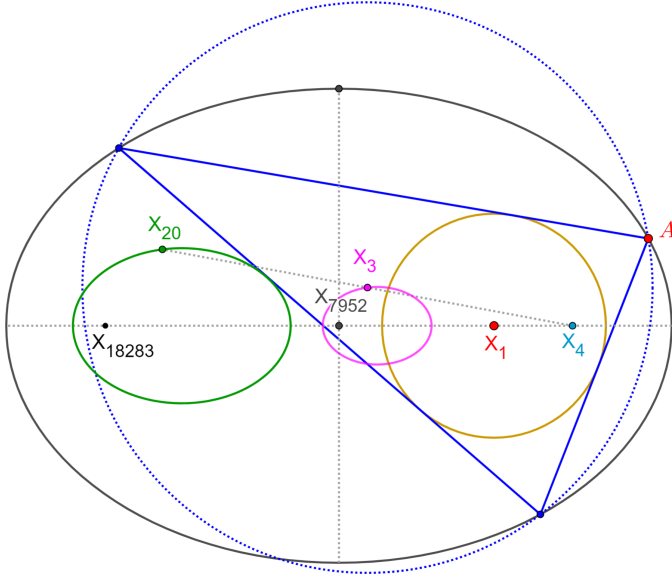


FIGURE 27. The focal- X_4 family: the outer ellipse E has foci on X_4 and X_{18283} and center on X_{7952} . Also shown are the loci of the orthocenter X_3 , with a focus on said center, and that of the de Longchamps point X_{20} (a reflection of X_4 on X_3), so twice as big, and with a focus on the other focus of E . [Video](#)

Proof. The incenter-orthocenter squared distance is given by [36, Incenter, eqn.(6)]:

$$(3) \quad |X_1 - X_4|^2 = 2r^2 + 4R^2 - \frac{\sum l_i^2}{2} = 2r^2 + r_{pol}^2$$

Since for this family $|X_1 X_4|$ is fixed as is the inradius r . The actual expression was obtained by CAS-based simplification. \square

Referring to Figure 28 (left):

Definition 2. The MacBeath Poncelet family is inscribed in a circle and circumscribes the MacBeath inconic, with foci at the circumcenter and its isogonal conjugate, the orthocenter. Its center is the Euler center X_5 , the midpoint of X_3 and X_4 [36, MacBeath inconic].

For the purposes of this section, let a, b denote the semiaxis' lengths of the MacBeath inconic.

Lemma 4. *Over the MacBeath family, the sum of squared sidelengths, the sum of double-angle cosines, and the product of cosines are conserved. There are given by:*

$$\begin{aligned} \sum l_i^2 &= 9R^2 - |X_3 - X_4|^2 = 32a^2 + 4b^2 \\ \sum \cos(2\theta_i) &= \frac{c^2 - 3a^2}{2a^2} \\ \prod \cos \theta_i &= \frac{\sum l_i^2}{8R^2} - 1 = \frac{b^2}{8a^2} \end{aligned}$$

Proof. The first relation is direct from [36, Circumcenter, eqn.(6)], noting that the (i) the circumradius R is fixed and (ii) the caustic foci X_3, X_4 are stationary. The

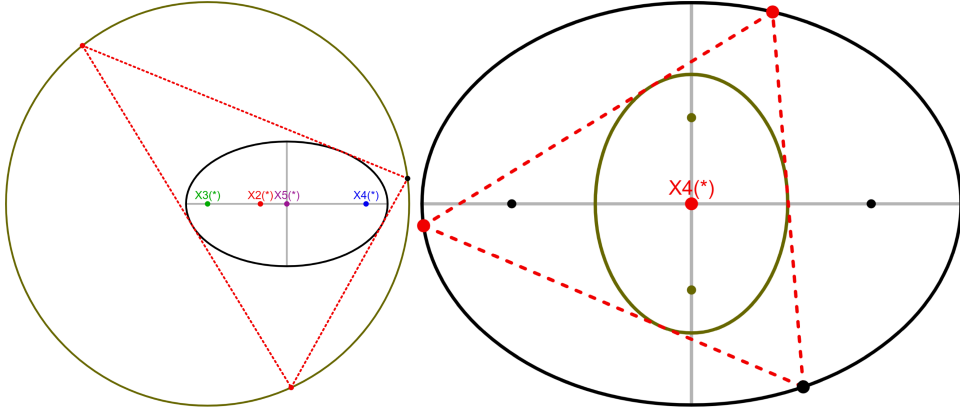


FIGURE 28. **left:** the ‘MacBeath’ family, [live](#); **right:** the ‘dual’ family, [live](#).

second one is obtained via CAS-simplification. The third one is direct from [36, Circumradius, eqn.(5)]. \square

Referring to Figure 28 (right):

Definition 3. The *dual* Poncelet family is interscribed between two dual ellipses [35]. They are also homothetic if one is rotated by 90-degrees.

Proposition 29. *The (i) MacBeath and (ii) dual families conserve $r_{pol}^2 < 0$. These are given by:*

$$r_{pol,macbeath}^2 = \frac{|X_3 - X_4|^2 - R^2}{2} = -2b^2$$

$$r_{pol,dual}^2 = -\frac{a^2b^2}{a^2 + b^2}$$

Proof. The first is direct from $|X_3 - X_4|^2 = 9R^2 - \sum l_i^2 = 2r_{pol}^2 + R^2$ [36, Orthocenter, eqn.(14)], noting that the MacBeath circumradius R is fixed and the caustic foci X_3 and X_4 are stationary. For the dual family, X_4 is stationary at the common center. Given the first relation it would therefore be sufficient to prove that $|X_3(t)|^2 - R^2(t)$ is constant. The final expression is obtained via CAS simplification. \square

Observation 12. *For the dual family the locus of the circumcenter X_3 is an ellipse homothetic to E with factor $c^2/(2(a^2 + b^2))$.*

Conjecture 4. *A Poncelet triangle family maintains X_4 stationary only if the conics are configured as focal- X_4 , MacBeath or Dual.*

7.4. Iso- $\mathbf{X}(7)$. Referring to Figure 25 (bottom right):

Proposition 30. *For the circular caustic with center and radius given by:*

$$C_7 = \left[\frac{k_7}{2a}, 0 \right], \quad r_7 = \frac{b^2}{2a}$$

The Gergonne point will be stationary at:

$$X_7 = \left[\frac{2ak_7}{4a^2 - b^2}, 0 \right]$$

where $k_7 = \sqrt{4a^4 - 5a^2b^2 + b^4}$.

Observation 13. *The iso- X_7 family is the polar image of the Brocard porism [25, 31] with respect to the circumcircle, i.e., its tangential triangle. The former's stationary Gergonne point X_7 coincides with the stationary symmedian point X_6 of the Brocard porism [9].*

Proposition 31. *The family conserves the sum of half-angle tangents, given by:*

$$\sum_{i=1}^3 \tan \frac{\theta_i}{2} = \frac{\sqrt{4a^2 - b^2}}{a}$$

The $N > 3$ generalization of the Brocard porism is known as the Harmonic family, studied [12].

Conjecture 5. *The sum of half-angle tangents is also conserved for the polar image of the Harmonic family, for all $N > 3$.*

Since X_7 is stationary, the quantity $|X_1X_7|$ will also be conserved. For a generic triangle with semiperimeter s , this is given by [23, Corollary 4.2]:

$$|X_1 - X_7|^2 = r^2 \left(1 - \frac{3s^2}{(r + 4R)^2} \right)$$

Proposition 32. *Over Iso- X_7 triangles, this reduces to:*

$$|X_1 - X_7|^2 = \frac{b^4 c^2}{4a^2(4a^2 - b^2)}$$

Definition 4. The Adams circle of a triangle is centered on X_1 and has radius R_A given by [36, Adams Circle]:

$$R_A = \frac{r\sqrt{\rho^2 - l_1 l_2 l_3 s - \rho s^2}}{\rho - s^2}$$

where $\rho = l_1 l_2 + l_2 l_3 + l_3 l_1$ and s is the semi-perimeter.

Proposition 33. *The Iso- X_7 family conserves R_A and its value is given by:*

$$R_A = \frac{b^2}{2a} \sqrt{\frac{5a^2 - b^2}{4a^2 - b^2}}$$

ACKNOWLEDGEMENTS

We would like to thank Arseniy Akopyan, Clark Kimberling, Peter Moses, and Richard Schwartz, for commenting on our developing results, encouraging us constantly, and providing insights and formulas. The second author is fellow of CNPq and coordinator of Project PRONEX/ CNPq/ FAPEG 2017 10 26 7000 508.

APPENDIX A. AFFINE TRIPLES

Triples α, β, γ used to express a given triangle center X_k as the linear combination $\alpha X_1 + \beta X_2 + \gamma X_3$, where $\rho = r/R$, reproduced from [17, Table 1]:

	X_1	X_2	X_3	X_4	X_5	X_7	X_8	X_9	X_{10}	X_{11}	X_{12}	X_{20}	X_{21}	X_{35}	X_{36}	X_{40}	X_{46}
α	1	0	0	0	0	$\frac{2\rho+4}{\rho+4}$	-2	$\frac{-\rho-2}{\rho+4}$	$-\frac{1}{2}$	$\frac{1}{1-2\rho}$	$\frac{1}{1+2\rho}$	0	0	$\frac{1}{2\rho+1}$	$\frac{1}{1-2\rho}$	-1	$\frac{1+\rho}{1-\rho}$
β	0	1	0	3	$\frac{3}{2}$	$\frac{3\rho}{\rho+4}$	3	$\frac{6}{\rho+4}$	$\frac{3}{2}$	$\frac{-3\rho}{1-2\rho}$	$\frac{3\rho}{1+2\rho}$	-3	$\frac{3}{2\rho+3}$	0	0	0	0
γ	0	0	1	-2	$-\frac{1}{2}$	$-\frac{4\rho}{\rho+4}$	0	$\frac{2\rho}{\rho+4}$	0	$\frac{\rho}{1-2\rho}$	$\frac{-\rho}{1+2\rho}$	4	$\frac{2\rho}{2\rho+3}$	$\frac{2\rho}{2\rho+1}$	$\frac{-2\rho}{1-2\rho}$	2	$\frac{-2\rho}{1-\rho}$

	X_{55}	X_{56}	X_{57}	X_{63}	X_{65}	X_{72}	X_{78}	X_{79}	X_{80}	X_{84}	X_{90}	X_{100}	X_{104}	X_{119}
α	$\frac{1}{1+\rho}$	$\frac{1}{1-\rho}$	$\frac{2+\rho}{2-\rho}$	$\frac{-\rho-2}{\rho+1}$	$\rho+1$	$-\rho-2$	$\frac{\rho+2}{\rho-1}$	1	$\frac{2\rho+1}{1-2\rho}$	$\frac{-\rho-2}{\rho}$	$\frac{-(\rho+1)^2}{\rho^2+2\rho-1}$	$\frac{2}{2\rho-1}$	$\frac{-2}{2\rho-1}$	$\frac{1}{2\rho-1}$
β	0	0	0	$\frac{3}{\rho+1}$	0	3	$\frac{-3}{\rho-1}$	$\frac{6\rho}{2\rho+3}$	$\frac{-6\rho}{1-2\rho}$	$\frac{6}{\rho}$	$\frac{6\rho}{\rho^2+2\rho-1}$	$\frac{-3}{2\rho-1}$	$\frac{3}{2\rho-1}$	$\frac{3\rho-3}{2\rho-1}$
γ	$\frac{\rho}{1+\rho}$	$\frac{-\rho}{1-\rho}$	$\frac{-2\rho}{2-\rho}$	$\frac{2\rho}{\rho+1}$	$-\rho$	ρ	0	$\frac{-6\rho}{2\rho+3}$	$\frac{2\rho}{1-2\rho}$	$\frac{2\rho-4}{\rho}$	$\frac{2\rho(\rho-1)}{\rho^2+2\rho-1}$	$\frac{2\rho}{2\rho-1}$	$\frac{2\rho-2}{2\rho-1}$	$\frac{-\rho+1}{2\rho-1}$

	X_{140}	X_{142}	X_{144}	X_{145}	X_{149}	X_{153}	X_{165}	X_{191}	X_{200}
α	0	$\frac{\rho+2}{2\rho+8}$	$\frac{-4\rho-8}{\rho+4}$	$\frac{4}{7}$	$\frac{-4}{6\rho-3}$	$\frac{4}{6\rho-3}$	$-\frac{1}{3}$	-1	$\frac{\rho+4}{\rho-2}$
β	$\frac{3}{4}$	$\frac{3\rho+6}{2\rho+8}$	$\frac{12-3\rho}{\rho+4}$	$\frac{3}{7}$	$\frac{-6\rho+9}{6\rho-3}$	$\frac{-6\rho-3}{6\rho-3}$	0	$\frac{6}{2\rho+3}$	$\frac{-6}{\rho-2}$
γ	$\frac{1}{4}$	$\frac{-2\rho}{2\rho+8}$	$\frac{8\rho}{\rho+4}$	0	$\frac{12\rho-8}{6\rho-3}$	$\frac{12\rho-4}{6\rho-3}$	$\frac{4}{3}$	$\frac{4\rho}{2\rho+3}$	0

APPENDIX B. LOCUS BEHAVIORS

Proposition 34. Over Poncelet triangles with a circular caustic, from X_1 to X_{1000} , X_k sweep a conic locus for the following k : 2, 3, 4, 5, 7, 8, 10, 11, 12, **20**, 35, 36, 40, 42, 46, 55, 56, 57, 65, 79, 80, 81, **140**, 145, 165, 171, 174, 176, 202, 213, 226, 354, 355, 365, 366, 367, 368, 370, **376**, **381**, **382**, 388, 390, 396, 482, 484, 495, 496, 497, 498, 499, 506, 507, **546**, **547**, **548**, **549**, **550**, 551, 553, 554, 559, 588, 590, 593, 597, 605, 609, 611, 612, **631**, **632**, 938, 939, 940, 941, 942, 944, 946, 950, 954, 955, 962, 975, 977, 980, 981, 989, 999, 1000.

Note that boldfaced entries above are triangle centers which are fixed combinations of X_2 and X_3 and will, over any Poncelet pair, sweep a conic locus [17].

Amongst some of the above-listed centers, six types of “locus behaviors” are observed:

- (1) **\mathcal{E} -homothety:** X_k , $k = 2$ (see [30]), 4, 8 (concentric), 10, 145, 368, 370, 551, 944, 946 are homothetic to \mathcal{E} .
- (2) **Axis alignment:** X_k , $k = 7, 79, 390, 1000$ are axis-aligned with E but not homothetic to it.
- (3) **C-focus:** X_k , $k = 5, 12, 355, 495, 496$ have C for a focus.
- (4) **C-major:** the major axis of X_k , $k = 3$ (foci on E 's axes), 35, 40, 55, 165 pass through C .
- (5) **C-minor:** the minor axis of X_k $k = 46, 56, 57, 999$ pass through C .
- (6) **Circle:** X_k , $k = 11$ (on incircle), 36, 65, 80 (centered on C), 354, 484, 942 are circles.

Pictures of the above can be found in [24].

APPENDIX C. THE CONTACT FAMILY

We now consider phenomena of the family of *contact triangles* of the incircle-circumscribed Poncelet analyzed above, i.e., with vertices at the tangents of each side with the incircle. Referring to Figure 29, the contact family is Ponceletian: it is circle-inscribed and envelops the polar image of tangents to \mathcal{E} with respect to the incircle, also a conic [1].

Let T_o be a triangle inscribed in the unit circle, and \mathcal{E}_c an inconic with foci f, g , written as complex numbers. Referring to Figure 30:

Lemma 5. A Poncelet family of triangles inscribed in the unit circle and circumscribing an ellipse with foci $f, g \in \mathbb{C}$ contains an equilateral triangle iff $1/f + 1/g$ is on the unit circle.

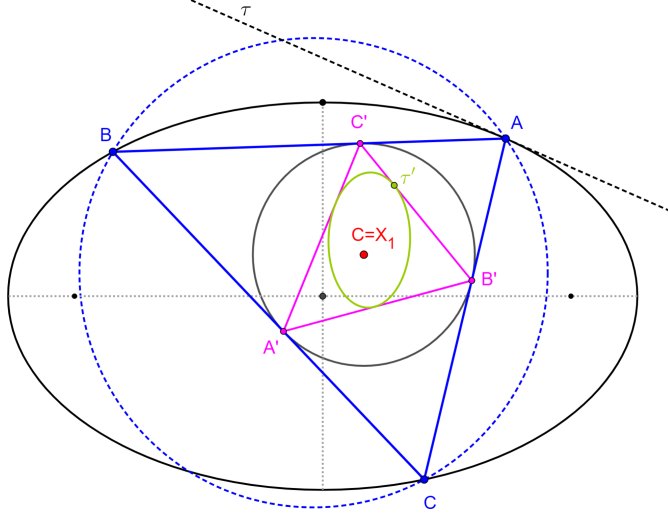


FIGURE 29. The contact family $A'B'C'$ is circle-inscribed and envelopes a conic which is the polar image of tangents τ to \mathcal{E} with respect to the incircle. The point τ' indicated the instantaneous polarity.

Proof. to do First, assume that T_o is an equilateral triangle in this family. Let $\zeta \in \mathbb{T}$ be one of the vertices of T_o so that the other vertices are $e^{\frac{2\pi}{3}i}\zeta$ and $e^{\frac{4\pi}{3}i}\zeta$. Using the symmetric parameterization described in [Theorem 1](#), let $\lambda_o \in \mathbb{T}$ be the parameter corresponding to triangle T_o . Plugging in the vertices in the parameterization, we get

$$\begin{aligned} f + g + \lambda_o \bar{f} \bar{g} &= \zeta + e^{\frac{2\pi}{3}i}\zeta + e^{\frac{4\pi}{3}i}\zeta = \zeta \left(1 + e^{\frac{2\pi}{3}i} + e^{\frac{4\pi}{3}i}\right) = 0 \\ z_1 z_2 + z_2 z_3 + z_3 z_1 &= fg + \lambda(\bar{f} + \bar{g}) \\ z_1 z_2 z_3 &= \lambda \end{aligned}$$

□

Henceforth, let \mathcal{T}_o^* denote a Poncelet family of triangles interscribed between the unit circle and some inconic \mathcal{E}_c satisfying [Lemma 5](#).

Definition 5. A triangle's *Kiepert parabola* is tangent to the three sides of a triangle. Its focus is X_{110} , always on the circumcircle, and its directrix is the Euler line $X_2 X_3$ [\[36\]](#).

Still referring to Figure 30:

Proposition 35. Over \mathcal{T}_o^* , X_{110} is stationary at $(1/f + 1/g)^{-1}$.

Proof. to do

□

On [\[18\]](#), (i) the midpoint of X_3 and X_{110} is called X_{1511} , and (ii) X_{3233} is the vertex of the Kiepert inparabola [\[20\]](#). Referring to [Figure 31](#):

Observation 14. Over \mathcal{T}_o^* , X_{3233} sweeps a circle with diameter $X_{110}X_{1511}$, i.e., 1/2.

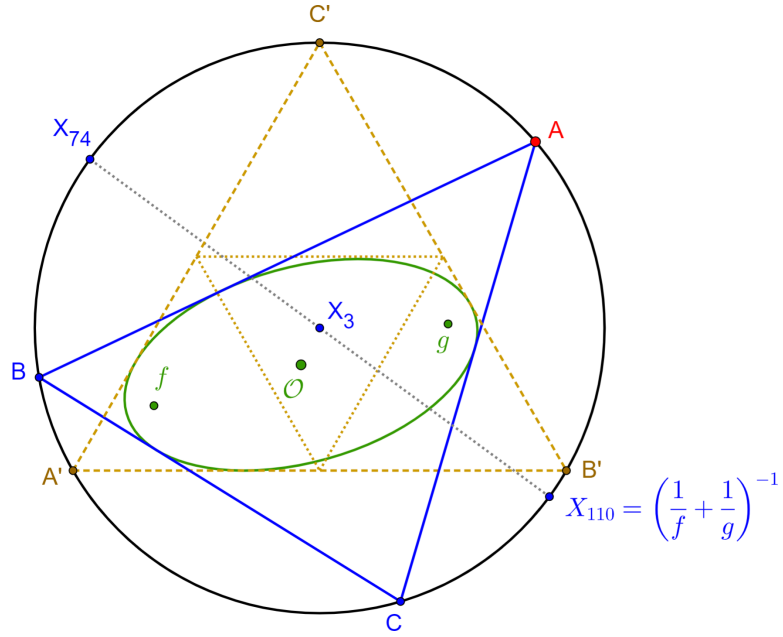


FIGURE 30. $T'_o = A'B'C'$ (brown) is an equilateral for which an inconic (green), centered at \mathcal{O} , is chosen, with foci at (complex) f, g . ABC is a triangle (blue) in the Poncelet family defined by the circumcircle (black) and the chosen inconic. Over the family, X_{110} , the focus of the Kiepert parabola (not shown) is stationary at $(1/f + 1/g)^{-1}$, as is its antipode X_{74} . [Video](#)

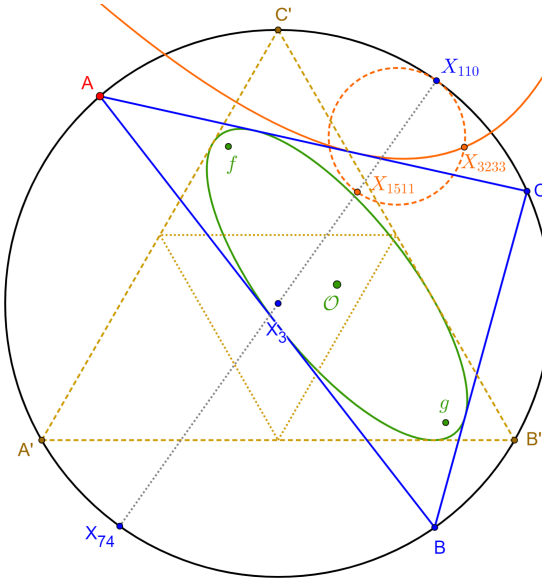


FIGURE 31. A $T_o = ABC$ in \mathcal{T}_o (blue) is shown (blue) along with its Kiepert parabola (orange), also an inconic, with focus at X_{110} . Over \mathcal{T}_o , the locus of its vertex X_{3233} is a circle (dashed orange) whose diameter is $X_{110}X_{1511}$. [Video](#)

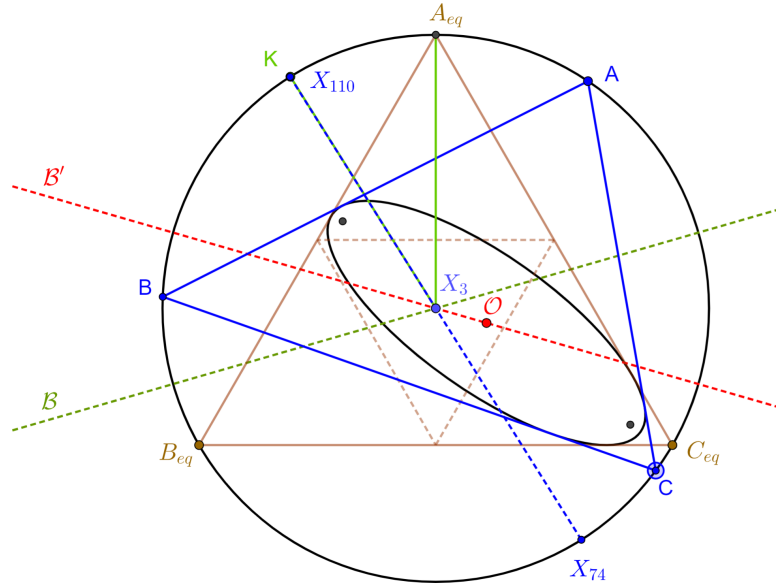


FIGURE 32. The construction in Proposition 36: K is chosen on the circumcircle; A_{eq} is a vertex of the equilateral; $T_o = ABC$ is a Poncelet triangle in \mathcal{T}_o^* ; \mathcal{B} (dashed green) is the external bisector of $\angle KX_3A_{eq}$; \mathcal{B}' (dashed red) is its reflection about X_3A_{eq} ; over all caustic centers \mathcal{O} on \mathcal{B}' , X_{110} is stationary, over \mathcal{T}_o^* , at the chosen K .

Referring to Figure 32, let A_{eq} be one of the vertices of the equilateral in T_o^* . Let K be a chosen point on the circumcircle. Let \mathcal{B} represent the external bisector of $\angle KX_3A_{eq}$.

Proposition 36. Over \mathcal{T}_o^* , X_{110} will be stationary at K for any \mathcal{O} on the reflection of \mathcal{B} about X_3A_{eq} .

Proof. to do

Referring to Figure 33, let $T_o = ABC$ be some generic triangle. Let \mathcal{O} be the center of an inconic \mathcal{E}_c . Let \mathcal{T}_o be the Poncelet family defined by the circumcircle and \mathcal{E}_c . Let \mathcal{L}_{35} be the perpendicular bisector of X_3X_5 .

Proposition 37. T_o will contain an equilateral iff \mathcal{O} lies on \mathcal{L}_{35} . Furthermore, the stationary X_{110} is independent of \mathcal{O} .

Proof. to do

Let $\alpha = \angle X_{110}X_3\mathcal{O}$. Let \mathcal{O}' be the counterclockwise rotation of \mathcal{O} about X_3 by $\alpha/3 + \pi$. Still referring to Figure 33,

Proposition 38. *One vertex of the equilateral contained in T_o is located at the intersection of X_3O' with the circumcircle.*

Proof. to do

Let \mathcal{T}'_o be the family of tangential triangles to \mathcal{T}_o , i.e., whose sides are tangent to the circumcircle at the vertices of \mathcal{T}_o [36, Tangential Triangle]. Clearly, this family circumscribes a circle and will be inscribed in an ellipse \mathcal{E} , called above \mathcal{T} .

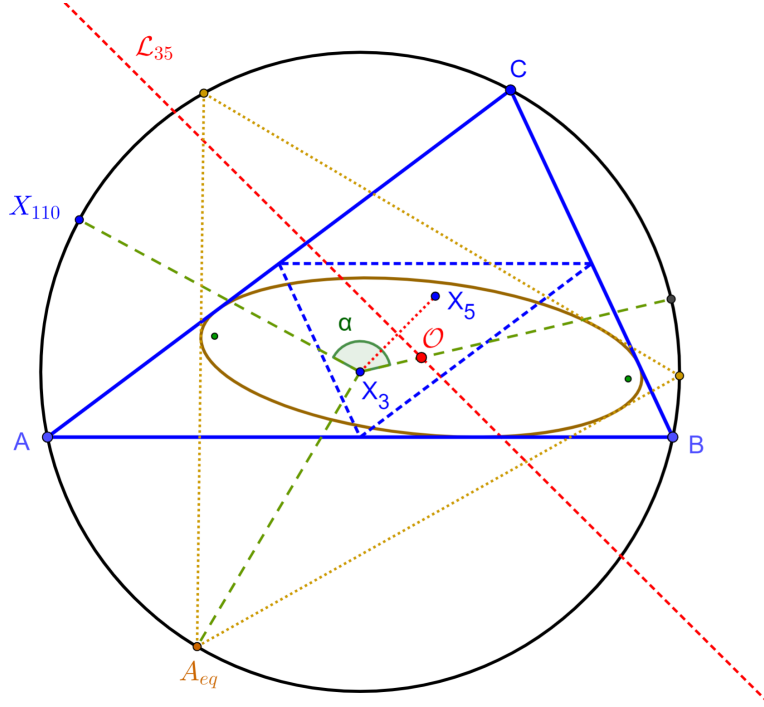


FIGURE 33. The construction of Propositions 37 and 38. X_{110} (of $T_o = ABC$) is stationary over Poncelet if \mathcal{O} lies on \mathcal{L}_{35} (dashed red), the perpendicular bisector of X_3 and X_5 . A vertex A_{eq} of the equilateral contained in the family is shown.

Observation 15. \mathcal{E} is the polar image of the chosen inconic with respect to the circumcircle.

Corollary 12. Since the tangential of an equilateral is an equilateral, \mathcal{T}'_o will contain an equilateral, and therefore the center of its incircle will be on \mathcal{E}_{eq} .

In turn, this leads to a restatement of Proposition 15:

Corollary 13. The Feuerbach point X_{11} of \mathcal{T}'_o will be stationary.

Proof. X_{110} of a reference triangle is X_{11} of its tangential. Conversely, X_{11} of the reference is X_{110} of the contact triangle. \square

On [18], X_{65} is the orthocenter X_4 of the contact triangle.

Corollary 14. The locus of X_{65} of the tangential family is a circle.

Proof. The contact family is Poncelet (sides envelop the polar image of \mathcal{E} wrt incircle) and circle-inscribed. X_4 is always homothetic to a 90-degree-rotated version of the inscribing conic. \square

APPENDIX D. SEMIAxes OF THE $X(7)$ LOCUS

Let (xc, yc) represent the center of the circular caustic. The square of the major semiaxis length a_7 of the X_7 locus is given by:

$$\begin{aligned}
& (a^*b^2*(16*a^17*(b^4+22*b^2*y_c^2+9*y_c^4)+16*a*b^12*x_c^2*(b^2-y_c^2)*(28*b^4-30*x_c^2*y_c^2+28*y_c^4-b^2*(51*x_c^2+56*y_c^2))+8*a^15*(35*b^6-36*x_c^2*y_c^4-2*b^4*(4*x_c^2+175*y_c^2)-3*b^2*(44*x_c^2*y_c^2+119*y_c^4))+a^13*(-2559*b^8+144*x_c^4*y_c^4+b^6*(-812*x_c^2+2517*y_c^2)+3*b^4*(32*x_c^4+2168*x_c^2*y_c^2)+4945*y_c^4)+3*b^2*(352*x_c^4*y_c^2+812*x_c^2*y_c^4+189*y_c^6))+a^3*b^10*(64*b^8+60*x_c^6*y_c^2-1212*x_c^4*y_c^4+832*x_c^2*y_c^6)+64*y_c^8-64*b^6*(73*x_c^2*y_c^2)+12*b^4*(573*x_c^4+848*x_c^2*y_c^2+32*y_c^4)-b^2*(141*x_c^6+6960*x_c^4*y_c^2+6336*x_c^2*y_c^4+256*y_c^6))+a^11*b^2*(2698*b^8+b^6*(5397*x_c^2+18490*y_c^2))+18*b^4*(42*x_c^4-983*x_c^2*y_c^2-1409*y_c^4)-4*x_c^2*y_c^2*(88*x_c^4-105*x_c^2*y_c^2+81*y_c^4)-b^2*(64*x_c^6+4608*x_c^4*y_c^2+15699*x_c^2*y_c^4+2226*y_c^6))+a^5*b^8*(112*b^8+8*b^6*(1545*x_c^2-22*y_c^2)-3*b^4*(4991*x_c^4+11960*x_c^2*y_c^2+48*y_c^4)+b^2*(138*x_c^6+22881*x_c^4*y_c^2+23064*x_c^2*y_c^4+368*y_c^6)+4*(3*x_c^8+18*x_c^6*y_c^2-75*x_c^4*y_c^4+114*x_c^2*y_c^6-40*y_c^8))-a^7*b^6*(3876*b^8+b^6*(383*x_c^2-6744*y_c^2))-6*b^4*(1897*x_c^4+6571*x_c^2*y_c^2-288*y_c^4)+3*b^2*(-85*x_c^6+9530*x_c^4*y_c^2+14813*x_c^2*y_c^4+424*y_c^6)+4*(7*x_c^8+171*x_c^6*y_c^2-756*x_c^4*y_c^4+483*x_c^2*y_c^6-33*y_c^8))+a^9*b^4*(9097*b^8-b^6*(14218*x_c^2+26815*y_c^2)+b^4*(-3105*x_c^4+300*x_c^2*y_c^2+14943*y_c^4)+b^2*(-196*x_c^6+15861*x_c^4*y_c^2+39894*x_c^2*y_c^4+2811*y_c^6)+4*(4*x_c^8+226*x_c^6*y_c^2-639*x_c^4*y_c^4+354*x_c^2*y_c^6-9*y_c^8))-192*b^11*x_c^2*(b^2-y_c^2)^2*d-128*a^14*b^2*(b^2+3*y_c^2)*d+192*a^12*b^2*(2*b^4+4*x_c^2*y_c^2+3*y_c^4+b^2*(2*x_c^2+23*y_c^2))*d-4*a^2*b^9*(80*b^6-75*x_c^4*y_c^2+144*x_c^2*y_c^4-80*y_c^6-120*b^4*(7*x_c^2+2*y_c^2)+3*b^2*(79*x_c^4+232*x_c^2*y_c^2+80*y_c^4))*d+12*a^10*b^2*(258*b^6-32*x_c^4*y_c^2+33*x_c^2*y_c^4-b^4*(79*x_c^2+1116*y_c^2))-2*b^2*(16*x_c^4+193*x_c^2*y_c^2+211*y_c^4))*d+12*a^4*b^7*(168*b^6+5*x_c^6-99*x_c^4*y_c^2+178*x_c^2*y_c^4-48*y_c^6-2*b^4*(577*x_c^2+192*y_c^2)+b^2*(263*x_c^4+1320*x_c^2*y_c^2+264*y_c^4))*d-12*a^6*b^5*(47*b^6+15*x_c^6-90*x_c^4*y_c^2+102*x_c^2*y_c^4-25*y_c^6-b^4*(1130*x_c^2+799*y_c^2)+b^2*(232*x_c^4+2404*x_c^2*y_c^2+777*y_c^4))*d-4*a^8*b^3*(2579*b^6-32*x_c^6-54*x_c^4*y_c^2+129*x_c^2*y_c^4+9*y_c^6+3*b^4*(31*x_c^2-447*y_c^2))-3*b^2*(62*x_c^4+1570*x_c^2*y_c^2+949*y_c^4))*d))/((a^2-b^2)^2*(16*a^6-9*b^4*x_c^2-8*a^4*(b^2+2*x_c^2-y_c^2))*(-(a^2*b^2*(8*b^2+x_c^2-24*y_c^2))+a^4*(b^2-9*y_c^2)+16*(b^6-b^4*y_c^2))^2)
\end{aligned}$$

where: $d = \sqrt{(a^4 - a^2*x_c^2 + b^2*x_c^2)*(b^4 + a^2*y_c^2 - b^2*y_c^2)}$. The expression for the minor semi-axis b_7 is the above where (a, b) and (x_c, y_c) are permuted.

APPENDIX E. TABLE OF SYMBOLS

symbol	meaning
$\mathcal{E}, \mathcal{E}_c$	Poncelet conics (incidence and tangency)
a, b, c	semi-axis' and half-focal lengths of \mathcal{E}
a_c, b_c, c_c	idem for \mathcal{E}_c
$\mathcal{K}, C = (x_c, y_c)$	incircle and its center ($= X_1$)
T, l_i, θ_i	a Poncelet triangle, sidelengths, and internal angles
r, R	inradius and circumradius of a T
$\mathcal{E}_{eq}, a_{eq}, b_{eq}$	(elliptic) locus of \mathcal{E} -inscr. equilat. centroids and semi-axes
X_k	triangle center indexed in Kimberling's [18]
X_1	Incenter: meet of angle bisectors
X_2	Barycenter: meet of medians
X_3	Circumcenter: meet of perpendicular bisectors
X_4	Orthocenter: meet of altitudes
X_5	Center of Euler's (9-pt) circle
X_7	Gergonne point: perspector of the contact triangle
X_8	Nagel's point: perspector of the extouch triangle
X_{11}	Feuerbach's point: touchpoint of incircle and Euler's circle
X_{36}	circumcircle-inverse of X_1
X_{59}	isogonal conjugate of X_{11}
X_{80}	reflection of X_1 on X_{11}
$C_i = (x_i, y_i), a_i, b_i$	center and semiaxes of the (elliptic) locus of X_i 's
F_i, F'_i	foci of the (elliptic) locus of X_i
X_i^*	stationary X_i
\mathcal{T}	Poncelet triangle family about the incircle
\mathcal{L}_k	locus of X_k over \mathcal{T}
\mathcal{T}^*	the family \mathcal{T} containing an equilateral
\mathcal{T}_g	Poncelet triangle interscribed between two generic conics
\mathcal{T}_o	circle-inscribed Poncelet triangle family
\mathcal{T}_o^*	the family \mathcal{T}_o containing and equilateral
\mathcal{T}'_o	tangential triangles to \mathcal{T}_o^* , identical to \mathcal{T}^*
f, g	foci of caustic of \mathcal{T}_o
λ	parameter of symmetric parametrization [4]

TABLE 2. Symbols used in the article. For geometric constructions for the X_i , see [36].

REFERENCES

- [1] Akopyan, A. V., Zaslavsky, A. A. (2007). *Geometry of Conics*. Providence, RI: Amer. Math. Soc. 31
- [2] Bellio, F., Garcia, R., Reznik, D. (2022). Parabola-inscribed Poncelet polygons derived from the bicentric family. *J. Croatian Soc. for Geom. & Gr. (KoG)*, 26. 26

- [3] del Centina, A. (2016). Poncelet's porism: a long story of renewed discoveries i. *Arch. Hist. Exact Sci.*, 70(2): 1–122. doi.org/10.1007/s00407-015-0163-y. 2
- [4] Daapp, U., Gorkin, P., Shaffer, A., Voss, K. (2019). *Finding Ellipses: What Blaschke Products, Poncelet's Theorem, and the Numerical Range Know about Each Other*. MAA Press/AMS. 2, 6, 37
- [5] Darlan, I., Reznik, D. (2021). An app for visual exploration, discovery, and sharing of Poncelet 3-periodic phenomena. 5
- [6] Davis, P. J. (1995). The rise, fall, and possible transfiguration of triangle geometry: A mini-history. *Am. Math. Monthly*, 102(3): 204–214. 5
- [7] Dragović, V., Radnović, M. (2011). *Poncelet Porisms and Beyond: Integrable Billiards, Hyperelliptic Jacobians and Pencils of Quadrics*. Frontiers in Mathematics. Basel: Springer. books.google.com.br/books?id=Qc0mDAEACAAJ. 2, 5
- [8] Fierobe, C. (2021). On the circumcenters of triangular orbits in elliptic billiard. *J. Dyn. Control Syst.* [doi:10.1007/s10883-021-09537-2](https://doi.org/10.1007/s10883-021-09537-2). 2
- [9] Garcia, R., Reznik, D. (2021). Family ties: Relating Poncelet 3-periodics by their properties. *J. Croatian Soc. for Geom. & Gr. (KoG)*, 25(25): 3–18. <https://hrcak.srce.hr/en/clanak/390431>. 10, 30
- [10] Garcia, R., Reznik, D. (2024). The conic locus of the isogonal conjugate of a point with respect to generic Poncelet triangles. *TBD*. In preparation. 17, 19
- [11] Garcia, R., Reznik, D., Koiller, J. (2023). Loci of 3-periodics in an elliptic billiard: why so many ellipses? *J. Symb. Computation*, 114(4): 336–358. 2, 17, 23
- [12] Garcia, R., Reznik, D., Roitman, P. (2022). New properties of harmonic polygons. *J. Geom. Graphics*, 26(2): 41–60. 30
- [13] Georgiev, V., Nedylkova, V. (2012). Poncelet's porism and periodic triangles in ellipse. *Dynamat*. www.dynamat.oriw.eu/upload_pdf/20121022_153833_0.pdf. 2
- [14] Glutsyuk, A. (2014). On odd-periodic orbits in complex planar billiards. *J. Dyn. Control Syst.*, 20(3): 293–306. doi.org/10.1007/s10883-014-9236-5. 2
- [15] Helman, M., Garcia, R., Reznik, D. (2024). Locus of the orthocenter over generic Poncelet triangles. *TBD*. In preparation. 8
- [16] Helman, M., Laurain, D., Garcia, R., Reznik, D. (2021). Invariant center power and loci of Poncelet triangles. *J. Dyn. & Contr. Sys.* 5, 6, 23
- [17] Helman, M., Laurain, D., Reznik, D., Garcia, R. (2022). Poncelet triangles: a theory for locus ellipticity. *Beitr. Algebra Geom.* 2, 4, 7, 30, 31
- [18] Kimberling, C. (2019). Encyclopedia of triangle centers. faculty.evansville.edu/ck6/encyclopedia/ETC.html. 2, 4, 10, 14, 15, 19, 21, 26, 27, 32, 35, 37
- [19] Kimberling, C. (2020). Central lines of triangle centers. bit.ly/34vVoJ8. 15
- [20] Moses, P. (2024). Vertex of the Kiepert inparabola. Private Communication. 32
- [21] Odehnal, B. (2011). Poristic loci of triangle centers. *J. Geom. Graph.*, 15(1): 45–67. 2, 3, 23, 26
- [22] Ogilvy, C. S. (1969). *Excursions in Geometry*. New York: Oxford Univ. Press. 20
- [23] Queiroz, J. F. (2021). Gergonne's point and outstanding distances. Romanian Mathematical Magazine. <https://www.ssmrmh.ro/wp-content/uploads/2021/07/GERGONNES-POINT-AND-OUTSTANDING-DISTANCES.pdf>. Florică Anastase (ed.). 30
- [24] Reznik, D. (2024). Six nifty behaviors of loci of Poncelet triangles with a circular caustic. ResearchGate. https://www.researchgate.net/publication/382637554_Six_nifty_behaviors_of_loci_of_Poncelet_triangles_with_a_circular_caustic. 31
- [25] Reznik, D., Garcia, R. (2022). A matryoshka of Brocard porisms. *European J. of Math.*, 8: 308–329. 30
- [26] Reznik, D., Garcia, R., Koiller, J. (2020). The ballet of triangle centers on the elliptic billiard. *J. Geom. Graphics*, 24(1): 079–101. 2, 17
- [27] Reznik, D., Garcia, R., Koiller, J. (2020). Can the elliptic billiard still surprise us? *Math Intelligencer*, 42: 6–17. rdcu.be/b2cg1. 3
- [28] Roitman, P., Garcia, R., Reznik, D. (2021). New invariants of Poncelet-Jacobi bicentric polygons. *Arnold Math. J.*, 7(4): 619–637. 26
- [29] Romaskevich, O. (2014). On the incenters of triangular orbits on elliptic billiards. *Enseign. Math.*, 60(3-4): 247–255. arxiv.org/pdf/1304.7588.pdf. 2, 23
- [30] Schwartz, R., Tabachnikov, S. (2016). Centers of mass of Poncelet polygons, 200 years after. *Math. Intelligencer*, 38(2): 29–34. www.math.psu.edu/tabachni/prints/Poncelet5.pdf. 8, 31

- [31] Shail, R. (1996). Some properties of brocard points. *The Mathematical Gazette*, 80(489): 485–491. [30](#)
- [32] Sirfoga, U. (2014). Equilateral triangle inscribed in a ellipse. Mathematics Stack Exchange. math.stackexchange.com/q/769819. [12](#)
- [33] Skutin, A. (2013). On rotation of a isogonal point. *J. of Classical Geom.*, 2: 66–67. jcgeometry.org/Articles/Volume2/JCG2013V2pp66-67.pdf. [17](#)
- [34] Stanev, M. (2019). Locus of the centroid of the equilateral triangle inscribed in an ellipse. *International Journal of Computer Discovered Mathematics (IJCDM)*, 4: 54–65. [4](#), [12](#)
- [35] Walker, R. J. (1978). *Algebraic Curves*. New York: Springer. [29](#)
- [36] Weisstein, E. (2019). Mathworld. *MathWorld—A Wolfram Web Resource*. mathworld.wolfram.com. [4](#), [7](#), [9](#), [17](#), [21](#), [22](#), [26](#), [27](#), [28](#), [29](#), [30](#), [32](#), [34](#), [37](#)